trophic adipocytes in situations of excess energy. In the context of obesity-related diseases including insulin resistance and diabetes, inhibition of p21 in adipocytes might have a therapeutic effect by suppressing adipose tissue expansion. However, it is also possible p21-mediated adipocyte differentiation is important for proper storage of excess lipids in adipose tissue, thereby protecting against ectopic lipid storage and insulin resistance. Further studies are needed to clarify the precise mechanism by which p53/p21 pathway is regulated and involved in obesity and insulin resistance in adipose tissue. Recent reports on another CDK inhibitor, p27, as well as Skp2, the F-box protein that controls ubiquitin-mediated degradation of p27, implicates the Skp2/p27 pathway in determining the cell number of adipocytes and pancreatic β cells (5, 22, 38–40). Mice that lack CDK4 develop insulin-dependent diabetes as a result of a reduction in islet mass, whereas deletion of p27 ameliorates hyperglycemia in diabetic mice by maintaining compensatory islet hyperplasia and hyperinsulinemia, suggesting that these factors are involved in cell cycle regulation and could also play a role in β cell mass and function (38, 41). However, p21 did not have a significant impact on β cell function in our study (supplemental Table A3) as recently reported (42). Taken together, these data implicate p21 in controlling adipocyte cell size and p27 in determining cell number, reflecting distinct regulations and adipose tissue growth by both of the major CDK inhibitors.

In conclusion, our data demonstrate that p21 plays dual roles in both adipocyte differentiation through cell cycle arrest and in adipocyte hypertrophy through its anti-apoptotic action. Via these mechanisms mutually connected, p21 supports adipose tissue expansion during obesity linking to insulin resistance. Our data suggest that a cell cycle regulator can be involved in a wide range of physiology and pathophysiology in adipocytes, providing a new link between cell growth and metabolism.

Acknowledgments—We are grateful to Drs. Hiroshi Sakaue and Takehiro Nakamura for analysis of adipocyte cell size by Coulter counter. We thank Yuko Tamai for management of mice.

REFERENCES

1. Gregoire, F. M., Smas, C. M., and Sul, H. S. (1998) *Physiol. Rev.* **78,** 783–809
2. Rosen, E. D., and Spiegelman, B. M. (2000) *Annu. Rev. Cell Dev. Biol.* **16,** 145–171
3. Morrison, R. F., and Farmer, S. R. (1999) *J. Biol. Chem.* **274,** 17088–17097
4. Nakae, J., Kitamura, T., Kitamura, Y., Biggs, W. H., III, Arden, K. C., and Accili, D. (2003) *Dev. Cell* **4,** 119–129
5. Sakai, T., Sakaue, H., Nakamura, T., Okada, M., Matsuki, Y., Watanabe, E., Hiramatsu, R., Nakayama, K., Nakayama, K. I., and Kasuga, M. (2007) *J. Biol. Chem.* **282,** 2038–2046
6. Spiegelman, B. M., and Flier, J. S. (2001) *Cell* **104,** 531–543
7. Harper, J. W., Adami, G. R., Wei, N., Keyomarsi, K., and Elledge, S. J. (1993) *Cell* **75,** 805–816
8. el-Deiry, W. S., Tokino, T., Velculescu, V. E., Levy, D. B., Parsons, R., Trent, J. M., Lin, D., Mercer, W. E., Kinzler, K. W., and Vogelstein, B. (1993) *Cell* **75,** 817–825
9. Xiong, Y., Hannon, G. J., Zhang, H., Casso, D., Kobayashi, R., and Beach, D. (1993) *Nature* **366,** 701–704
10. Noda, A., Ning, Y., Venable, S. F., Pereira-Smith, O. M., and Smith, J. R. (1994) *Exp. Cell Res.* **211,** 90–98
11. Hunter, T. (1993) *Cell* **75,** 839–841
12. Polyak, K., Waldman, T., He, T. C., Kinzler, K. W., and Vogelstein, B. (1996) *Genes Dev.* **10,** 1945–1952
13. Inoue, N., Shimano, H., Nakakuki, M., Matsuzaka, T., Nakagawa, Y., Yamamoto, T., Sato, R., Takahashi, A., Sone, H., Yahagi, N., Suzuki, H., Toyoshima, H., and Yamada, N. (2005) *Mol. Cell. Biol.* **25,** 8938–8947
14. Shimomura, I., Hammer, R. E., Richardson, J. A., Ikemoto, S., Bashmakov, Y., Goldstein, J. L., and Brown, M. S. (1998) *Genes Dev.* **12,** 3182–3194
15. Yahagi, N., Shimano, H., Matsuzaka, T., Najima, Y., Sekiya, M., Nakagawa, Y., Ide, T., Tomita, S., Okazaki, H., Tamura, Y., Iizuka, Y., Ohashi, K., Gotoda, T., Nagai, R., Kimura, S., Ishibashi, S., Osuga, J., and Yamada, N. (2003) *J. Biol. Chem.* **278,** 25395–25400
16. Yahagi, N., Shimano, H., Matsuzaka, T., Sekiya, M., Najima, Y., Okazaki, S., Okazaki, H., Tamura, Y., Iizuka, Y., Inoue, N., Nakagawa, Y., Takeuchi, Y., Ohashi, K., Harada, K., Gotoda, T., Nagai, R., Kadowaki, T., Ishibashi, S., Osuga, J., and Yamada, N. (2004) *J. Biol. Chem.* **279,** 20571–20575
17. Ide, T., Shimano, H., Yahagi, N., Matsuzaka, T., Nakakuki, M., Yamamoto, T., Nakagawa, Y., Takahashi, A., Suzuki, H., Sone, H., Toyoshima, H., Fukamizu, A., and Yamada, N. (2004) *Nat. Cell Biol.* **6,** 351–357
18. Nakagawa, Y., Shimano, H., Yoshikawa, T., Ide, T., Tamura, M., Furusawa, M., Yamamoto, T., Inoue, N., Matsuzaka, T., Takahashi, A., Hasty, A. H., Suzuki, H., Sone, H., Toyoshima, H., Yahagi, N., and Yamada, N. (2006) *Nat. Med.* **12,** 107–113
19. Okazaki, H., Osuga, J., Tamura, Y., Yahagi, N., Tomita, S., Shionoiri, F., Iizuka, Y., Ohashi, K., Harada, K., Kimura, S., Gotoda, T., Shimano, H., Yamada, N., and Ishibashi, S. (2002) *Diabetes* **51,** 3368–3375
20. Brugarolas, J., Chandrasekaran, C., Gordon, J. I., Beach, D., Jacks, T., and Hannon, G. J. (1995) *Nature* **377,** 552–557
21. Maeda, N., Shimomura, I., Kishida, K., Nishizawa, H., Matsuda, M., Nagaretani, H., Furuyama, N., Kondo, H., Takahashi, M., Arita, Y., Komuro, R., Ouchi, N., Kihara, S., Tochino, Y., Okutomi, K., Horie, M., Takeda, S., Aoyama, T., Funahashi, T., and Matsuzawa, Y. (2002) *Nat. Med.* **8,** 731–737
22. Naaz, A., Holsberger, D. R., Iwamoto, G. A., Nelson, A., Kiyokawa, H., and Cooke, P. S. (2004) *FASEB J.* **18,** 1925–1927
23. Hirsch, J., and Gallian, E. (1968) *J. Lipid Res.* **9,** 110–119
24. Cushman, S. W., and Salans, L. B. (1978) *J. Lipid Res.* **19,** 269–273
25. Yamada, T., Katagiri, H., Ishigaki, Y., Ogihara, T., Imai, J., Uno, K., Hasegawa, Y., Gao, J., Ishihara, H., Niijima, A., Mano, H., Aburatani, H., Asano, T., and Oka, Y. (2006) *Cell Metab.* **3,** 223–229
26. Oda, K., Arakawa, H., Tanaka, T., Matsuda, K., Tanikawa, C., Mori, T., Nishimori, H., Tamai, K., Tokino, T., Nakamura, Y., and Taya, Y. (2000) *Cell* **102,** 849–862
27. Berberich, S. J., Litteral, V., Mayo, L. D., Tabesh, D., and Morris, D. (1999) *Differentiation* **64,** 205–212
28. Constance, C. M., Morgan, J. I. T., and Umek, R. M. (1996) *Mol. Cell. Biol.* **16,** 3878–3883
29. Shieh, S. Y., Ahn, J., Tamai, K., Taya, Y., and Prives, C. (2000) *Genes Dev.* **14,** 289–300
30. Craig, A. L., Blaydes, J. P., Burch, L. R., Thompson, A. M., and Hupp, T. R. (1999) *Oncogene* **18,** 6305–6312
31. Okuno, A., Tamemoto, H., Tobe, K., Ueki, K., Mori, Y., Iwamoto, K., Umesono, K., Akanuma, Y., Fujiwara, T., Horikoshi, H., Yazaki, Y., and Kadowaki, T. (1998) *J. Clin. Investig.* **101,** 1354–1361
32. Prins, J. B., Niesler, C. U., Winterford, C. M., Bright, N. A., Siddle, K., O'Rahilly, S., Walker, N. I., and Cameron, D. P. (1997) *Diabetes* **46,** 1939–1944
33. Cram, E. J., Ramos, R. A., Wang, E. C., Cha, H. H., Nishio, Y., and Firestone, G. L. (1998) *J. Biol. Chem.* **273,** 2008–2014
34. Gartel, A. L., and Tyner, A. L. (1999) *Exp. Cell Res.* **246,** 280–289
35. Ashcroft, M., Kubbutat, M. H., and Vousden, K. H. (1999) *Mol. Cell. Biol.* **19,** 1751–1758
36. Merched, A. J., and Chan, L. (2004) *Circulation* **110,** 3830–3841

37. Heron-Milhavet, L., Franckhauser, C., Rana, V., Berthenet, C., Fisher, D., Hemmings, B. A., Fernandez, A., and Lamb, N. J. (2006) *Mol. Cell. Biol.* **26,** 8267–8280
38. Uchida, T., Nakamura, T., Hashimoto, N., Matsuda, T., Kotani, K., Sakaue, H., Kido, Y., Hayashi, Y., Nakayama, K. I., White, M. F., and Kasuga, M. (2005) *Nat. Med.* **11,** 175–182
39. Auld, C. A., and Morrison, R. F. (2006) *Obesity (Silver Spring)* **14,** 2136–2144
40. Auld, C. A., Hopkins, R. G., Fernandes, K. M., and Morrison, R. F. (2006) *Biochem. Biophys. Res. Commun.* **346,** 314–320
41. Rane, S. G., Dubus, P., Mettus, R. V., Galbreath, E. J., Boden, G., Reddy, E. P., and Barbacid, M. (1999) *Nat. Genet.* **22,** 44–52
42. Cozar-Castellano, I., Haught, M., and Stewart, A. F. (2006) *Diabetes* **55,** 3271–3278

nature medicine

Crucial role of a long-chain fatty acid elongase, Elovl6, in obesity-induced insulin resistance

Takashi Matsuzaka[1,2], Hitoshi Shimano[1,2], Naoya Yahagi[2,3], Toyonori Kato[1], Ayaka Atsumi[1], Takashi Yamamoto[1], Noriyuki Inoue[1], Mayumi Ishikawa[1], Sumiyo Okada[1], Naomi Ishigaki[1], Hitoshi Iwasaki[1], Yuko Iwasaki[1], Tadayoshi Karasawa[1], Shin Kumadaki[1], Toshiyuki Matsui[1], Motohiro Sekiya[3], Ken Ohashi[3], Alyssa H Hasty[4], Yoshimi Nakagawa[1,2], Akimitsu Takahashi[1], Hiroaki Suzuki[1], Sigeru Yatoh[1], Hirohito Sone[1], Hideo Toyoshima[1], Jun-ichi Osuga[3] & Nobuhiro Yamada[1]

Insulin resistance is often associated with obesity and can precipitate type 2 diabetes. To date, most known approaches that improve insulin resistance must be preceded by the amelioration of obesity and hepatosteatosis. Here, we show that this provision is not mandatory; insulin resistance and hyperglycemia are improved by the modification of hepatic fatty acid composition, even in the presence of persistent obesity and hepatosteatosis. Mice deficient for *Elovl6*, the gene encoding the elongase that catalyzes the conversion of palmitate to stearate, were generated and shown to become obese and develop hepatosteatosis when fed a high-fat diet or mated to leptin-deficient *ob/ob* mice. However, they showed marked protection from hyperinsulinemia, hyperglycemia and hyperleptinemia. Amelioration of insulin resistance was associated with restoration of hepatic insulin receptor substrate-2 and suppression of hepatic protein kinase C ε activity resulting in restoration of Akt phosphorylation. Collectively, these data show that hepatic fatty acid composition is a new determinant for insulin sensitivity that acts independently of cellular energy balance and stress. Inhibition of this elongase could be a new therapeutic approach for ameliorating insulin resistance, diabetes and cardiovascular risks, even in the presence of a continuing state of obesity.

Insulin resistance is associated with obesity and is the major pathogenic indicator of early stages of type 2 diabetes. Epidemiological studies have shown that intake of excess saturated fatty acids is the principal lifestyle-related cause of insulin resistance and obesity-related diseases, including metabolic syndrome[1]. In general, it has been thought that dietary saturated fatty acids are detrimental, monounsaturated fatty acids are neutral and polyunsaturated fatty acids are beneficial, although intracellular events mediated by these fatty acids have not been fully characterized. During high-fat diet feeding, the influx of free fatty acids results in the accumulation of triglycerides, promoting a lipotoxic state, and this induces insulin resistance in skeletal muscle, adipose tissue and liver[2]. Intracellular accumulation of fatty acids activates both oxidative degradation and incorporation of these fatty acids into triglycerides as a protective adaptation against their cytotoxicity. When these mechanisms are overwhelmed, fatty acids may activate proinflammatory and stress-responsive signals such as the nuclear factor-κB and c-Jun N-terminal kinase pathways. These events, in turn, inhibit insulin signaling through abnormal phosphorylation or degradation of insulin signaling molecules, leading to metabolic deterioration[3–6]. Recent data also suggest that the Janus kinase (JAK)-signal transducer and activator of transcription (STAT)-3–suppressor of cytokine signaling (SOCS)-3 pathway that mediates leptin signals is involved in insulin resistance and leptin resistance[7–9].

Lipogenesis is a key event in the energy storage system. The biosynthesis of fatty acids is sequentially catalyzed by the enzymes acetyl–coenzyme A (CoA) carboxylase, fatty acid synthase (FAS) and stearoyl-CoA desaturase (SCD)-1 (**Supplementary Fig. 1a** online). The entire pathway is controlled by the transcription factor sterol regulatory element–binding protein (SREBP)-1c (refs. 10–12). Saturated fatty acids, as well as high-carbohydrate diets, activate SREBP-1c and enhance lipogenesis[10,13]. Previously, we have shown that SREBP-1c inhibits insulin receptor substrate (IRS)-2 and contributes to insulin resistance in liver, implicating a link between lipogenesis and insulin resistance[14]. The elongation of long-chain fatty acids (ELOVL) family member 6 (Elovl6, also known as LCE and FACE) has been shown to be a target of SREBP-1 by microarray analysis of SREBP-1 transgenic mice, and it was predicted to be important for tissue fatty acid composition[15,16]. In this study, we have examined the effects of Elovl6 on obesity, hepatic steatosis and insulin resistance to better understand the roles of fatty acid composition in these obesity-related states.

[1]Department of Internal Medicine (Endocrinology and Metabolism) Graduate School of Comprehensive Human Sciences and [2]Center for Tsukuba Advanced Research Alliance University of Tsukuba, 1-1-1 Tennodai, Tsukuba Ibaraki 305-8575, Japan. [3]Department of Metabolic Disease, University of Tokyo, 7-3-1 Hongo, Bunkyo-ku, Tokyo 113-8655, Japan. [4]Department of Molecular Physiology and Biophysics, Vanderbilt University Medical Center, Nashville, Tennessee 37232, USA. Correspondence should be addressed to H.S. (shimano-tky@umin.ac.jp).

Received 24 May; accepted 28 August; published online 30 September 2007; doi:10.1038/nm1662

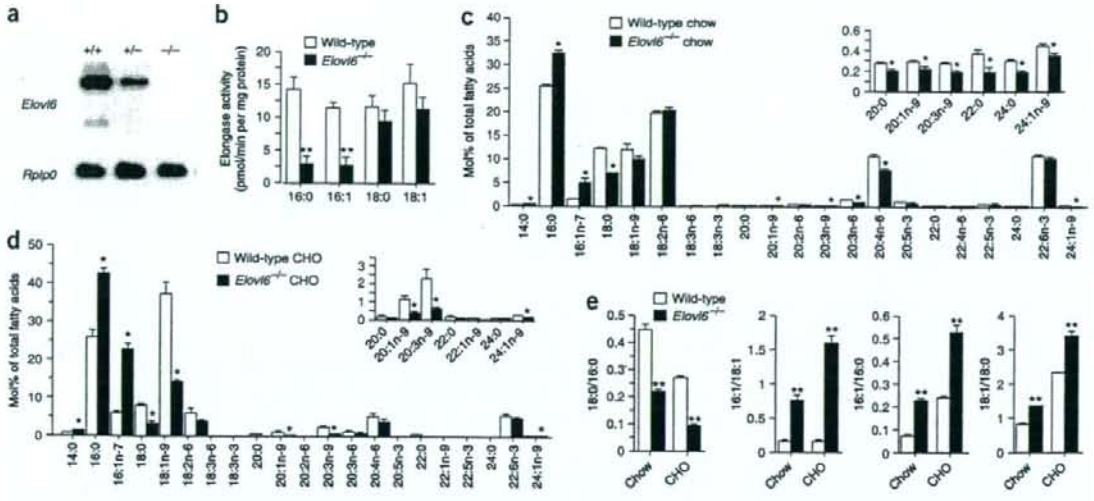

Figure 1 Targeting of the *Elovl6* gene. (**a**) Northern blot analysis of *Elovl6* expression in the livers of *Elovl6*$^{+/+}$, *Elovl6*$^{+/-}$ and *Elovl6*$^{-/-}$ mice. Total RNA (15 μg) pooled equally from three mice was subjected to northern blotting, followed by hybridization with the *Elovl6* cDNA. A cDNA probe for *Rplp0* (which encodes acidic ribosomal phosphoprotein P0) was used to confirm equal loading. (**b**) Assessment of Elovl6 enzymatic activity in liver total membrane fractions ($n = 5$ per group) using four separate substrates, 16:0-CoA, 16:1-CoA, 18:0-CoA and 18:1-CoA. (**c**,**d**) Fatty acid composition of liver tissue in wild-type and *Elovl6*$^{-/-}$ mice fed either a normal chow (**c**) or a CHO diet (**d**) for 2 weeks ($n = 3$–5 per group). (**e**) The ratio of stearate (18:0) to palmitate (16:0), palmitoleate (16:1n-7) to oleate (18:1n-9), 18:1 to 18:0 and 16:1 to 16:0 in livers of wild-type and *Elovl6*$^{-/-}$ mice. Results are represented as means ± s.e.m. $^{*}P < 0.05$, $^{**}P < 0.01$ for *Elovl6*$^{-/-}$ mice as compared to wild-type controls.

RESULTS

Metabolic features of *Elovl6*-null mice

The *Elovl6* gene product belongs to a highly conserved family of microsomal enzymes involved in the formation of long-chain fatty acids[17]. Functional analysis by expression experiments in cultured cells demonstrated that this enzyme has a role in the elongation of palmitate (16:0) to stearate (18:0), as well as in the elongation of palmitoleate (16:1n-7) to vaccinate (18:1n-7) (**Supplementary Fig. 1a**). To evaluate the importance of Elovl6 *in vivo*, *Elovl6*-null mice were created (**Supplementary Fig. 2a–c** online). Homozygous *Elovl6* knockout (*Elovl6*$^{-/-}$) mice had partial embryonic lethality, although surviving male and female mutants were fertile (**Supplementary Fig. 2d**). Gene disruption completely abolished hepatic *Elovl6* expression, resulting in an effective loss of its activity in the liver; this indicates that the hepatic elongase activity for these reactions is essentially attributable to Elovl6 (**Fig. 1a,b**). The residual elongase activity of palmitoleate to vaccinate in *Elovl6*$^{-/-}$ liver may be attributed to Elovl5, which has been reported to have a weak activity for this reaction[18]. To determine whether the livers of *Elovl6*$^{-/-}$ mice contained fewer C18 fatty acids, hepatic fatty acid composition was determined (**Fig. 1c,d**). Consistent with the absence of elongation of C16 fatty acids to C18, hepatic concentrations of stearate and oleate (18:1n-9) were lowered, whereas those of palmitate and palmitoleate were heightened, as compared to wild-type mice. These trends were more prominent in the livers of mice fed a fat-free, high-sucrose diet (CHO) that enhances endogenous hepatic fatty acid synthesis[10]. This increase was significant enough to make palmitoleate, which is usually a minor fatty acid class, the second most abundant fatty acid present in livers of CHO-fed mice (**Fig. 1d**). The ratios of 18:0/16:0 and 16:1/18:1, the markers of the elongase activity, were consistently decreased and increased, respectively, in the livers of *Elovl6*$^{-/-}$ mice as compared to wild-type controls (**Fig. 1e**). The ratios of 18:1/18:0 and 16:1/16:0, indicative of desaturation through SCD-1 activity, were apparently higher, although the expression of SCD-1 was decreased (**Fig. 1e**). These data confirm the importance of Elovl6 in maintaining the hepatic contents of 18:0 and 18:1 through *de novo* synthesis of these fatty acids, despite the abundance of 18:0 and 18:1 in the diet. The fatty acid composition of plasma followed the same trend as that of the liver, but changes were minimal in skeletal muscle and adipose tissue (**Supplementary Fig. 2**).

Elovl6$^{-/-}$ mice appeared grossly normal, although they were slightly, but significantly, leaner than wild-type littermates, despite an identical daily food intake of standard laboratory chow (**Fig. 2a–c**). However, there was no difference in the size or the appearance of adipocytes from white and brown adipose tissues (**Fig. 2d**). Postprandial plasma concentrations of insulin and leptin were lower in *Elovl6*$^{-/-}$ mice than in wild-type mice, whereas no significant changes were observed in the amounts of plasma glucose or lipid (**Fig. 2e** and **Supplementary Table 1** online). Hepatic total cholesterol and triglyceride levels were also not different between wild-type and *Elovl6*$^{-/-}$ mice on a chow diet (**Supplementary Table 1**). Because the *Elovl6*$^{-/-}$ mice had higher insulin sensitivity on a standard chow diet, we challenged these mice with a high-fat, high-sucrose diet (HF-HS) that is known to induce obesity, hepatosteatosis and insulin resistance[19]. This high-calorie diet markedly enhanced body weight gain in both wild-type and *Elovl6*$^{-/-}$ mice (which had identical daily food intakes) at a similar rate over the course of the study, although the slight, but significant, weight differences were sustained (**Fig. 2a–c**). Epididymal fat pad weight and total body fat percentage were markedly increased in both groups, with similar net increases (**Supplementary Table 1** and **Fig. 2b**). In accordance with the observed increase in adiposity, white and brown adipocytes were enlarged similarly in

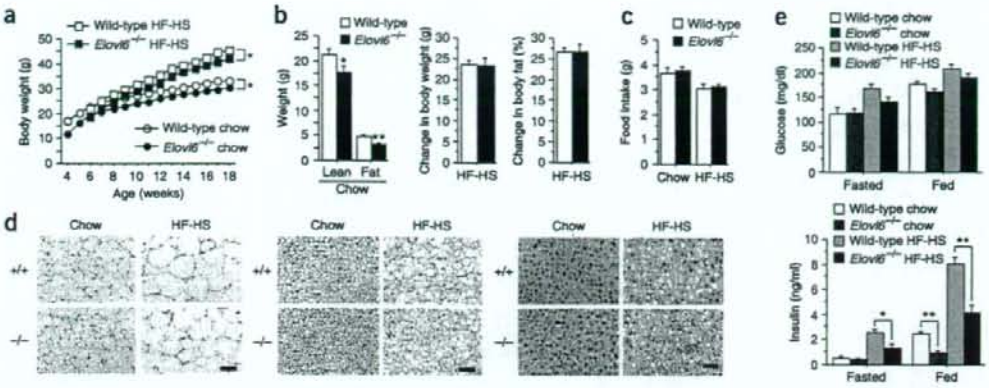

Figure 2 Body weight, adiposity and glucose homeostasis in wild-type and *Elovl6*$^{-/-}$ mice fed a standard chow or HF-HS diet. (**a**) Body weight changes of wild-type and *Elovl6*$^{-/-}$ mice fed a chow or HF-HS diet (n = 15–18 per group). Six-week-old male mice (n = 15–18) were fed a HF-HS diet for 12 weeks. (**b**) Average lean and fat mass and body weight and body fat gain by wild-type and *Elovl6*$^{-/-}$ mice fed a chow (n = 10 per group) or HF-HS diet (n = 8 per group). (**c**) Daily food intake in wild-type and *Elovl6*$^{-/-}$ mice provided *ad libitum* access to chow or HF-HS diet (n = 9–13 per group). (**d**) H&E-stained white adipose tissue (left), brown adipose tissue (middle) and liver (right) from wild-type and *Elovl6*$^{-/-}$ mice fed normal chow or HF-HS diet for 12 weeks. Scale bar, 50 μm. (**e**) Plasma glucose (left) and insulin (right) concentrations in wild-type (n = 18) and *Elovl6*$^{-/-}$ (n = 15) mice fed chow or HF-HS diet for 12 weeks. Results are represented as means ± s.e.m. $^{*}P < 0.05$, $^{**}P < 0.01$ for *Elovl6*$^{-/-}$ mice as compared to wild-type controls.

both groups after they had been fed the HF-HS diet (**Fig. 2d**). There were no obvious histological changes in white or brown adipose tissue; this included no observed change in the extent of mononuclear cell infiltration, which has been shown to contribute to proinflammatory response and insulin resistance in obesity[20,21]. There was a trend toward more severe hepatosteatosis in *Elovl6*$^{-/-}$ mice than in wild-type mice on the HF-HS diet, as estimated from hepatic triglyceride and cholesterol abundance as well as by histological staining (**Supplementary Table 1** and **Fig. 2d**). Overall, diet-induced obesity in *Elovl6*$^{-/-}$ mice was similar to that of normal controls.

Elovl6 deletion protects against diet-induced insulin resistance

Wild-type mice on the HF-HS diet exhibited a robust elevation in plasma insulin accompanied by slight increases in plasma glucose in both fasted and fed states, indicating the emergence of insulin resistance (**Fig. 2e**). However, *Elovl6*$^{-/-}$ mice on the HF-HS diet showed a significant reduction in plasma insulin compared to wild-type mice, in both nutritional states. The ameliorative effects of *Elovl6* deficiency on hyperinsulinemia was confirmed by a glucose tolerance test (GTT) (**Fig. 3a**). Wild-type mice on the HF-HS diet had markedly increased insulin abundance throughout the GTT. In contrast, HF-HS–fed *Elovl6*$^{-/-}$ mice exhibited a pattern of insulin response to glucose load nearly identical to that of mice on a chow diet. The protection from diet-induced insulin resistance in *Elovl6*$^{-/-}$ mice was more prominent during an insulin tolerance test (ITT) (**Fig. 3b**). Insulin sensitivity, as measured by the reduction in plasma glucose after insulin administration, was markedly reduced by the HF-HS diet in wild-type mice, whereas *Elovl6*$^{-/-}$ mice showed a nearly normal response to insulin. The area under the curve (AUC) of plasma insulin abundance during the GTT and the AUC of plasma glucose abundance during the ITT for the HF-HS–fed Elovl6$^{-/-}$ mice were significantly lower than those of the HF-HS–fed wild-type mice (**Fig. 3c,d**). A pattern of protection from insulin resistance similar to that observed in *Elovl6* deficiency was also observed in old (age 6–8 months) mice on a normal chow diet and in body weight–matched mice on the HF-HS diet (**Supplementary Fig. 3** online).

Chronic hyperinsulinemia due to insulin resistance is associated with hyperplasia and hypertrophy of islets caused by the adaptive proliferation of β-cells to maintain blood glucose levels. Histology of pancreatic sections demonstrated that there was no observable difference in islet morphology between the wild-type and *Elovl6*$^{-/-}$ mice on a chow diet (**Fig. 3e**). Wild-type mice fed a HF-HS diet showed a marked increase in the number and size of islets, suggesting an adaptive enlargement of β-cell mass in response to insulin resistance. In contrast, islet hypertrophy was essentially absent in *Elovl6*$^{-/-}$ pancreas, presumably because *Elovl6* deletion abrogated the development of diet-induced insulin resistance, despite the comparable obesity of the *Elovl6*$^{-/-}$ and wild-type mice.

Hepatic insulin signaling is preserved in *Elovl6*$^{-/-}$ mice

We studied insulin signaling in liver, muscle and white adipose tissue to estimate the contribution of these insulin-sensitive organs to the amelioration of diet-induced insulin resistance in *Elovl6*$^{-/-}$ mice (**Fig. 3f,g** and **Supplementary Fig. 4a** online). Insulin injection (5 units) induced phosphorylation of the major marker for insulin signaling, Akt (on Ser473), in each of these three tissues, with similar intensities in chow-fed wild-type and *Elovl6*$^{-/-}$ mice. In a reflection of their insulin resistance, wild-type mice on a HF-HS diet showed suppression of Akt phosphorylation in these organs, without alterations in total Akt protein concentration. *Elovl6* deficiency restored the suppressed Akt phosphorylation only in the liver. Thus, amelioration of whole body insulin resistance in *Elovl6*$^{-/-}$ mice can be attributed to restoration of hepatic insulin sensitivity. These data are consistent with the observation that changes in fatty acid composition were prominent only in the livers of *Elovl6*$^{-/-}$ mice (**Fig. 1c,d** and **Supplementary Fig. 2e–g**). Restoration of Akt phosphorylation was accompanied by increased total and phosphorylated IRS-2 protein in *Elovl6*$^{-/-}$ livers, whereas phosphorylation of the insulin receptor and IRS-1 remained

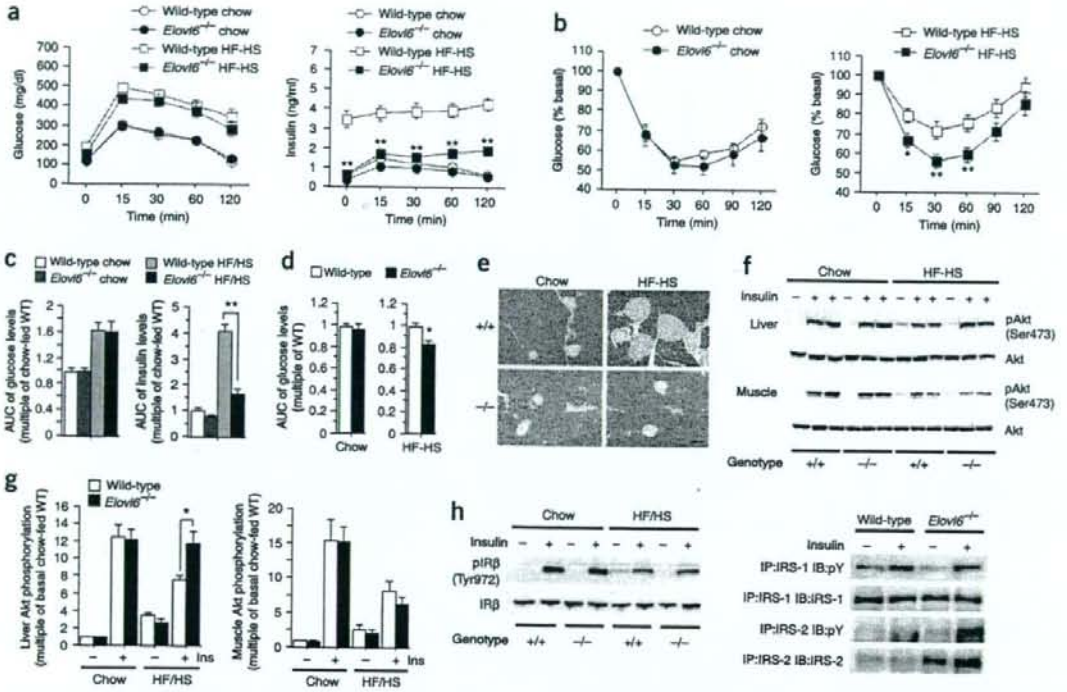

Figure 3 Protection from diet-induced insulin resistance in the absence of *Elovl6*. (**a**) Plasma glucose (left) and insulin (right) concentrations during intraperitoneal GTTs in wild-type and *Elovl6*$^{-/-}$ mice fed standard chow or HF-HS diets for 12 weeks ($n = 12$ per group). (**b**) ITTs in wild-type and *Elovl6*$^{-/-}$ mice fed standard chow (0.5 U insulin per kg of body weight; left) or HF-HS diet (1.0 U insulin per kg of body weight; right) ($n = 12$ per group). (**c**,**d**) The AUCs during the GTTs (**c**) or ITTs (**d**). WT, wild-type. (**e**) Protection of islet hyperplasia in *Elovl6*$^{-/-}$ mice fed a HF-HS diet. H&E-stained sections of pancreases from wild-type and *Elovl6*$^{-/-}$ mice fed standard chow or HF-HS diet. Scale bar, 50 μm. (**f**) Immunoblot analysis of Ser473-phosphoylated Akt (pAkt) and total Akt in response to a bolus injection of insulin in liver and skeletal muscle. Experiments were performed on mice fed a regular chow or HF-HS diet for 12 weeks. (**g**) Densitometric quantification of all livers and muscle immunoblot analysis from **f** ($n = 6$ per group). (**h**) Phosphorylation of insulin receptor β (pIRβ), IRS-1 and IRS-2 induced by a bolus injection of insulin was assessed in livers of wild-type and *Elovl6*$^{-/-}$ mice on a regular chow and/or HF-HS diet. Blots are representative of three independent experiments. IP, immunoprecipitated; IB, immunoblotted; pY, phosphorylated tyrosine. Results are represented as means ± s.e.m. $^{*}P < 0.05$, $^{**}P < 0.01$ for *Elovl6*$^{-/-}$ mice as compared to wild-type controls.

suppressed by the HF-HS diet in both genotypes (**Fig. 3h**), demonstrating that the restoration of insulin signaling in *Elovl6*$^{-/-}$ mice was mediated by the recovery of the hepatic IRS-2/Akt signaling pathway.

Recent studies have reported that stress or proinflammatory pathways such as the inhibitor of κB (IκB)-IκB kinase (IKK)-nuclear factor-κB, c-Jun N-terminal kinase and JAK–STAT-3–SOCS pathways impair insulin sensitivity, suggesting a link between inflammation and insulin resistance[3–9]. HF-HS feeding substantially regulated each of these pathways in the livers of wild-type mice contributing to insulin resistance (**Supplementary Fig. 4b**). Confoundingly, *Elovl6* deficiency tended to slightly activate these signals. It has recently been reported that SOCS proteins act as negative regulators in insulin signaling[7–9]. Contrary to what would be predicted from the observed amelioration-of-insulin-resistance phenotype, SOCS-3 (encoded by *Socs3*) and cytokine-inducible SH2-containing protein (*Cish*) were highly upregulated in *Elovl6*$^{-/-}$ livers (**Supplementary Fig. 4c**). Collectively, these data show that amelioration of insulin resistance by *Elovl6* deficiency is not mediated by suppression of these proinflammatory signals.

Gene expression in *Elovl6*$^{-/-}$ mice

To determine the molecular basis of these metabolic changes in the livers of *Elovl6*$^{-/-}$ mice, we examined the expression of genes involved in fatty-acid metabolism or glucose metabolism. Northern blot and real-time (RT) PCR analysis revealed that the HF-HS diet augmented hepatic expression of SREBP-1c (*Srebf1*) itself and of its target genes encoding lipogenic enzymes, including FAS (*Fasn*), Elovl6, SCD-1 (*Scd1*) and glycerol-3-phosphate acyltransferase (*Gpam*), in normal mice (**Fig. 4a**,**b**). The dietary induction of these genes was suppressed in *Elovl6*$^{-/-}$ mice. Consistently, expression of the nuclear active form of SREBP-1c protein was decreased (**Fig. 4c**). In contrast, expression of the forkhead box O1 and A2 proteins (Foxo1 and Foxa2), which have been reported to affect hepatic glucose and lipid metabolism[22,23], was diminished by the HF-HS diet, but was not changed in *Elovl6*$^{-/-}$ mice (**Fig. 4c**). In a reflection of better insulin sensitivity, nuclear exclusion of Foxo1 induced by insulin treatment was more detectable in *Elovl6*$^{-/-}$ mice than in wild-type mice (**Supplementary Fig. 4d**). Inhibition of *Scd1* expression caused by *Elovl6* deficiency was prominent in mice on both normal and HF-HS diets. As we have previously reported, activation of SREBP-1c directly represses IRS-2,

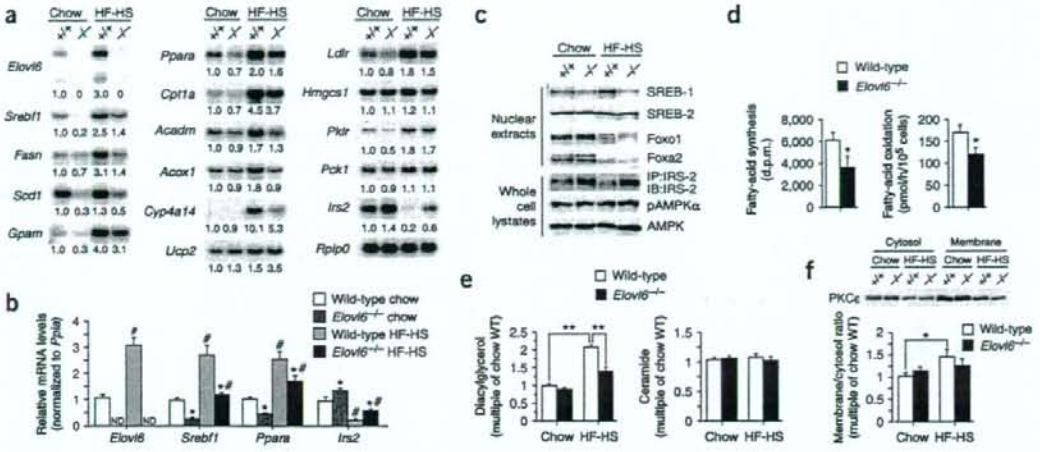

Figure 4 Effects of *Elovl6* deficiency on mRNA and protein levels and fatty acid metabolism in the livers of wild-type and *Elovl6*$^{-/-}$ mice fed a regular chow or HF-HS diet. (**a**,**b**) Northern blot (**a**) and RT-PCR (**b**) analysis of various mRNA levels in livers from wild-type and *Elovl6*$^{-/-}$ mice fed a standard chow or HF-HS diet for 12 weeks and sacrificed in a nonfasted state. (**a**) Total RNA was isolated from the livers of mice from each group ($n = 3$), pooled (15 μg) and subjected to northern blot analysis with the indicated cDNA probes. Fold changes of expression relative to chow-fed wild-type mice are shown. *Ucp2*, uncoupling protein-2; *Ldlr*, low-density lipoprotein receptor; *Hmgcs1*, hydroxymethylglutaryl-CoA synthase-1; *Pklr*, liver-type pyruvate kinase; *Pck1*, phosphoenolpyruvate carboxykinase-1, cytosolic. (**b**) Quantitative RT-PCR of RNA from livers of mice from each group ($n = 9$ per group). # indicates statistical significance between animals of the same genotype fed different diets, $P < 0.01$; * indicates statistical significance between wild-type and *Elovl6*$^{-/-}$ mice fed the same diet ($P < 0.05$). ND, not detectable. (**c**) Immunoblot analysis of SREBP-1, SREBP-2, Foxo1 and Foxa2 in nuclear extracts and IRS-2, Ser485-phosphorylated AMPKα (pAMPKα) and AMPKα in whole cell lysates from the livers of wild-type and *Elovl6*$^{-/-}$ mice fed a regular chow diet or HF-HS diet for 12 weeks. (**d**) The amount of fatty acid synthesis (left) and oxidation (right) in primary hepatocytes isolated from chow-fed wild-type and *Elovl6*$^{-/-}$ mice ($n = 9$ per group). d.p.m., decay per minute. (**e**) Diacylglycerol (left) and ceramide (right) content in the livers of wild-type and *Elovl6*$^{-/-}$ mice fed a regular chow diet or HF-HS diet for 12 weeks ($n = 6$ per group). (**f**) Immunoblot analysis determining membrane and cytosolic PKCε content in the livers of wild-type and *Elovl6*$^{-/-}$ mice fed a regular chow diet or HF-HS diet for 12 weeks ($n = 6$–8 per group). Blots are representative of three independent experiments. Results are represented as means ± s.e.m. *$P < 0.05$, **$P < 0.01$ for *Elovl6*$^{-/-}$ mice as compared to wild-type controls.

the main insulin signal mediator, and causes hepatic insulin resistance[14]. Therefore, suppression of SREBP-1c could contribute to the amelioration of hepatic insulin resistance in *Elovl6*$^{-/-}$ mice. Consistent with this notion, expression of *Irs2*, which was completely suppressed by the HF-HS diet in wild-type mice, was restored in the absence of *Elovl6* (**Fig. 4a–c**). Meanwhile, genes related to fatty acid oxidation that are regulated by nuclear receptor peroxisome proliferator–activated receptor (PPAR)α (*Ppara*), such as those encoding carnitine palmitoyltransferase-1 (*Cpt1a*), medium-chain acyl-CoA dehydrogenase (*Acadm*), acyl-CoA oxidase (*Acox1*) and cytochrome P450 4a14 (*Cyp4a14*), were induced by HF-HS diet in wild-type mice as an adaptive response (**Fig. 4a**). However, expression of these oxidation genes, including *Ppara*, was considerably decreased in *Elovl6*$^{-/-}$ mice, despite the amelioration of insulin resistance in these mice. AMP-activated protein kinase (AMPK) has been shown to facilitate energy expenditure and contribute to insulin sensitivity after treatment with biguanides, anti-diabetic agents that activate AMPK[24]. The amount of the active form of AMPKα (phosphorylated on Ser485) was not changed in *Elovl6*$^{-/-}$ livers (**Fig. 4c**). Thus, these data implicate that *Elovl6* deficiency suppressed both the synthesis and the degradation of fatty acids, resulting in a slightly increased hepatic triglyceride content. In support of this, fatty acid synthesis and oxidation were reduced in primary hepatocytes isolated from *Elovl6*$^{-/-}$ mice as compared to those from wild-type mice (**Fig. 4d**).

Diacylglycerol and ceramide have been thought to mediate insulin resistance in muscle and liver, accompanying accumulation of intracellular lipids[25–27]. We measured the contents of these lipid metabolites in the livers of wild-type and *Elovl6*$^{-/-}$ mice fed a chow or HF-HS diet (**Fig. 4e**). In wild-type mice, hepatic diacylglycerol content was elevated twofold by the HF-HS diet. *Elovl6* deficiency did not affect the basal level on a normal chow, but inhibited the induction by HF-HS diet observed in *Elovl6*$^{-/-}$ mice. No marked genotypic and dietary differences were evident in hepatic ceramide content. Diacylglycerol accumulation has been reported to be linked to the increased protein kinase C (PKC) ε activity and impaired phosphorylation of IRS-2 tyrosine induced by insulin[25,28]. Hepatic PKCε activity, as measured by the ratio of the amount of PKCε in cellular membranes to that in the cytosolic fraction, was significantly increased in the livers of HF-HS–fed wild-type mice, but not in *Elovl6*$^{-/-}$ mice (**Fig. 4f**), implying that the protection from diet-induced insulin resistance observed in *Elovl6*$^{-/-}$ mice could be mediated at least partially through this diacylglycerol-PKCε pathway.

Contribution of hepatic Elovl6 to insulin resistance

To estimate the importance of hepatic Elovl6 on whole-body insulin sensitivity, and to distinguish the long-term and short-term effects of an absence of *Elovl6*, we used adenoviral RNA interference (RNAi) to specifically inhibit hepatic expression of *Elovl6* (**Fig. 5a–e**). The *Elovl6* RNAi adenovirus (Elovl6i) robustly suppressed hepatic *Elovl6* expression and activity in C57BL6 mice on the HF-HS diet (**Fig. 5a**). Treatment with Elovl6i mimicked the hepatic changes observed in the liver of *Elovl6*$^{-/-}$ mice—it reduced expression of both *Srebf1* and *Ppara* and induced *Irs2* mRNA expression, and this was accompanied by a significant increase in hepatic triglycerides (**Fig. 5a,b**). Consequently,

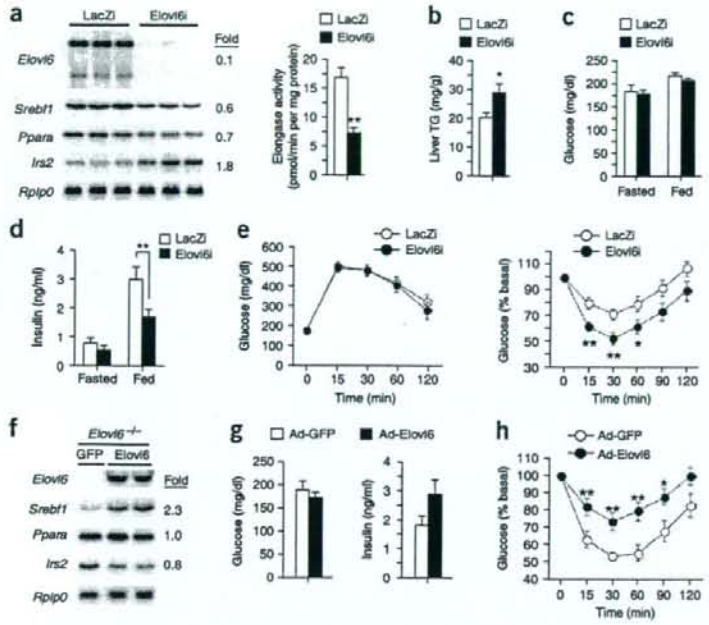

Figure 5 Effects of hepatic *Elovl6* expression on gene expression, fatty acid metabolism and insulin sensitivity. (**a–e**) Knockdown of hepatic *Elovl6* by adenoviral expression of RNAi. Eight-week-old male C57BL6 mice were fed a HF-HS diet for 2 weeks, followed by tail vein injection with adenovirus encoding RNAi targeting *Elovl6* (Elovl6i) or a *LacZ* (LacZi) control sequence. After 5–7 d of HF-HS feeding, mice were sacrificed in a nonfasted state. (**a**) Gene expression (left) and elongation activity (right) in the livers from LacZi and Elovl6i. The Elovl6i fold-change value is relative to the normalized value of LacZi control signal. (**b–d**) Liver trigyceride (**b**) plasma glucose (**c**) and plasma insulin (**d**) levels in a fasted or fed state. (**e**) GTT (left) and ITT (0.75 U insulin per kg body weight; right) in mice infected with either LacZi or Elovl6i. (**f–h**) Effect of adenovirus-mediated restoration of hepatic *Elovl6* expression in *Elovl6*$^{-/-}$ mice. Six-week-old male *Elovl6*$^{-/-}$ mice were fed a HF-HS diet for 4 weeks and then treated with adenovirus encoding GFP (control) or Elovl6 for 5–7 d. (**f**) Northern blot analysis of gene expression in the livers of *Elovl6*$^{-/-}$ mice injected with adenovirus encoding GFP (Ad-GFP) or Elovl6 (Ad-Elovl6). (**g**) Plasma glucose (left) and insulin (right) concentrations of the *Elovl6*$^{-/-}$ mice injected with Ad-GFP or Ad-Elovl6 in the fed state. (**h**) ITT in mice infected with either Ad-GFP or Ad-Elovl6 (0.75 U per kg body weight). Results are represented as means ± s.e.m., $n = 11–14$ per group. $^*P < 0.05$, $^{**}P < 0.01$ for experimental mice as compared with their respective controls.

knockdown of hepatic *Elovl6* significantly improved upon the increased plasma insulin level ($P < 0.01$) and impaired insulin sensitivity (as determined by ITT, $P < 0.01$) observed in mock-treated (LacZi), HF-HS–fed mice, even though there was no change in the plasma glucose level (**Fig. 5c–e**). Decreased plasma insulin was also observed by injecting Elovl6i into *ob/ob* (leptin-deficient, also known as *Lep*$^{-/-}$) mice (data not shown). Conversely, injection of a small amount of Elovl6 adenovirus (Ad-Elovl6) into *Elovl6*$^{-/-}$ animals fed a HF-HS diet caused hepatic expression of this enzyme to return to the control level (**Fig. 5f**). The restoration of *Elovl6* expression only in the liver canceled the protection from diet-induced hyperinsulinemia and insulin resistance in *Elovl6*$^{-/-}$ mice and was accompanied by increased *Srebf1* and decreased *Irs2* mRNA levels (**Fig. 5f–h**). In contrast, gene expression analysis in other energy organs, such as white fat, brown fat and skeletal muscle, in HF-HS–fed *Elovl6*$^{-/-}$ mice revealed no marked changes in the expression of genes involved in fatty acid oxidation, insulin sensitivity or lipogenesis, indicating that these organs do not contribute to the protection from insulin resistance noted in *Elovl6*$^{-/-}$ mice (**Supplementary Fig. 5a–c**). As an exception, *Fasn* expression was increased in these tissues. Insulin sensitivity was estimated in primary culture cells prepared from muscles of both groups (**Supplementary Fig. 5d**). There were no differences between wild-type and *Elovl6*$^{-/-}$ muscle cells in basal level, insulin-mediated induction or palmitate-mediated inhibition of glucose uptake (**Supplementary Fig. 5d**). Infection with Ad-Elovl6 did not restore the palmitate-suppressed uptake (**Supplementary Fig. 5d**). Thus, Elovl6 had no effects on the glucose uptake or insulin sensitivity of muscle cells. Taken together with the hepatic knockdown and restoration experiments, these data indicate that hepatic Elovl6 plays the major role in diet-induced insulin resistance.

To determine whether overexpression of *Elovl6* would affect hepatic gene expression and insulin signaling, mouse Hepa1c1c7 hepatoma cells were infected with Ad-Elovl6. *Elovl6* overexpression markedly induced SREBP-1c at both the mRNA and nuclear protein levels (**Fig. 6a**). Furthermore, activation of this enzyme blocked insulin-stimulated phosphorylation of Akt (**Fig. 6b**). Thus, hepatic Elovl6 activity could induce SREBP-1c expression and oppose insulin signaling.

To examine the physiological relevance of these data, we next asked whether insulin action and gene expression can be altered in liver cells as a function of the amount of cellular fatty acids regulated by Elovl6; we focused specifically on the effects of increasing the ratio of palmitoleate to palmitate. Hepa1c1c7 cells were cultured in medium supplemented with palmitate and with increasing concentrations of palmitoleate. Palmitate-alone treatment suppressed insulin-stimulated phosphorylation of Akt, and addition of palmitoleate restored it in a dose-dependent manner (**Fig. 6c**). *Srebf1* and *Ppara* mRNA expression were increased by palmitate treatment and were returned to the baseline by palmitate and palmitoleate supplementation, (**Fig. 6d**). These experiments showed that the cellular contents, or the ratio of palmitoleate to palmitate, could be a determinant for the hepatic insulin sensitivity regulated by Elovl6. These findings suggest that the fatty acid composition observed in the *Elovl6*$^{-/-}$ liver is favorable for insulin action.

Leptin signaling in *Elovl6* deficiency

Leptin is a key regulator of satiety and energy expenditure, thus determining energy metabolism and insulin sensitivity in the body[29]. Along with insulin resistance, diet-induced obesity by HF-HS was associated with leptin resistance, as evidenced by high plasma leptin levels and high leptin expression in adipose tissue in wild-type mice (**Supplementary Table 1** and **Supplementary Fig. 5a**). *Elovl6* deficiency improved leptin signaling, as judged by a marked decrease in plasma leptin in *Elovl6*$^{-/-}$ mice on both chow and HF-HS diets, irrespective of obesity. However, the food intake and resultant

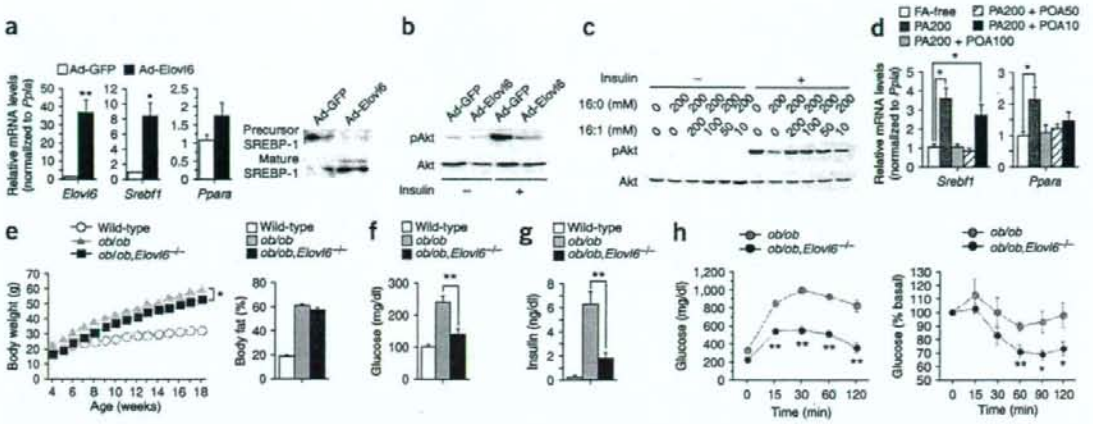

Figure 6 The effects of *Elovl6* overexpression and palmitate/palmitoleate ratio on Hepa1c1c7 hepatoma cells and of *Elovl6* deficiency on genetically obese mice. (**a**,**b**) Overexpression of *Elovl6* induces *Srebf1* expression and insulin resistance in hepatoma cells. (**a**) Gene expression in Hepa1c1c7 cells infected with adenovirus expressing either Ad-GFP ($n = 6$) or Ad-Elovl6 ($n = 6$), as estimated by RT-PCR analysis (left). Immunoblot analysis of SREBP-1 in membrane (precursor) and nuclear extracts (mature) from Hepa1c1c7 cells infected with adenovirus expressing either Ad-GFP or Ad-Elovl6 (right). Ad-GFP is used as a negative control. (**b**) *Elovl6* overexpression results in decreased Akt Ser473 phosphorylation in Hepa1c1c7 cells. Cells were stimulated with insulin for 10 min 16 h after adenovirus infection. (**c**,**d**) Effects of palmitate/palmitoleate ratio on Akt phosphorylation, **c**, and gene expression, **d**, in Hepa1c1c7 cells. Cells were supplemented with media alone (fatty acid–free) or media containing 200 μM palmitate (PA200), 200 μM palmitate + 200 μM palmitoleate (PA200 + POA200), 200 μM palmitate + 100 μM palmitoleate (PA200 + POA100), 200 μM palmitate + 50 μM palmitoleate (PA200 + POA50), or 200 μM palmitate + 10 μM palmitoleate (PA200 + POA10) for 16 h before insulin stimulation or RNA extraction. (**e**–**h**) Loss of *Elovl6* ameliorates insulin resistance in *ob/ob* mice. (**e**) Body weight changes (left) and body fat percentage (right) of wild-type ($n = 11$), *ob/ob* ($n = 11$) and *ob/ob,Elovl6*$^{-/-}$ mice ($n = 10$). (**f**,**g**) Plasma glucose (**f**) and insulin (**g**) concentrations in 6–8-week-old wild-type ($n = 11$), *ob/ob* ($n = 11$) and *ob/ob,Elovl6*$^{-/-}$ mice ($n = 10$). Mice were fasted for 24 h before experiments. (**h**) Plasma glucose levels during the GTT (left) and ITT (right) of 6–8-week-old *ob/ob* ($n = 9$) and *ob/ob,Elovl6*$^{-/-}$ ($n = 9$) mice. For ITT, insulin (2 U per kg body weight) was injected into each mouse after 6 h of fasting. Results are represented as means ± s.e.m. $^{*}P < 0.05$, $^{**}P < 0.01$ for experimental mice as compared with their respective controls.

adiposity did not change in *Elovl6*$^{-/-}$ mice on the HF-HS diet (**Fig. 2** and **Supplementary Table 1**). Livers from these mice did not show signs of the improved leptin signaling that was suppressed by HF-HS diet, as estimated by examining the amount of phosphorylation of STAT-3 and AMPK and fatty acid oxidation (**Supplementary Fig. 4b** and **Fig. 4a**). Furthermore, the effect of *Elovl6* deficiency was evaluated in *ob/ob* mice, which showed severe obesity, insulin resistance and diabetes (**Fig. 6e–h**). *ob/ob* and *Elovl6* double-mutant mice (*ob/ob, Elovl6*$^{-/-}$) showed sustained, severe obesity and had similar increases in body weight, body fat (**Fig. 6e**) and liver triglyceride content (data not shown) when compared to wild-type mice. However, insulin resistance and hyperglycemia were markedly less severe in the *ob/ob,Elovl6*$^{-/-}$ mice than in the *ob/ob* mice, as estimated by GTTs and ITTs conducted in mice 6–8 weeks (**Fig. 6f–h**) and 16–18 weeks (data not shown) of age. Taken together, these data imply that the effect of Elovl6 on insulin sensitivity is independent of leptin. The mechanism by which *Elovl6* deficiency decreases plasma leptin levels without changing adipocyte size is currently unknown, but must be related to enhanced insulin signaling.

DISCUSSION

Our current data establish the unique role of Elovl6 in hepatic lipogenesis. The major product of FAS, palmitate (16:0), is elongated by Elovl6 and desaturated by SCD-1 to yield oleic acid (18:1), the end product of mammalian fatty-acid synthesis. Recent studies in mouse models of ACC, FAS and SCD-1 deficiency, as well as our current data in *Elovl6*$^{-/-}$ mice, implicate various roles for endogenous fatty acid synthesis in energy metabolism (**Supplementary Fig. 1**). However, these deficiencies affect not only fatty acid synthesis, but also secondary activation of fatty acid oxidation. Liver-specific FAS knockout mice have phenotypes similar to those of PPARα-null mice, suggesting that some products of FAS are endogenous PPARα agonists that maintain fatty acid metabolism[30]. *Scd1*$^{-/-}$ mice are also protected from obesity and insulin resistance owing to activation of AMPK and fatty acid oxidation, implicating SCD-1 as a potential target for the treatment of diabetes[31,32]. Elovl6 and SCD-1 are structurally related and committed to consecutive reactions in lipogenesis; therefore, the improvement of insulin sensitivity in both knockout mice is not unexpected. It is possible that the decrease in *Scd1* expression could partly contribute to the insulin-sensitizing effect of *Elovl6* deficiency. However, in contrast to *Scd1*$^{-/-}$ mice, *Elovl6*$^{-/-}$ mice showed sustained obesity and low fatty acid oxidation in the liver, indicating that the mechanisms by which these two enzymes influence insulin sensitivity are not completely convergent. Thus, the conversion of palmitate to stearate is a key step in energy expenditure that discriminates between the physiological functions of Elovl6, a membrane-bound enzyme, and FAS, the multifunctional cytosolic enzyme that synthesizes fatty acids of up to 16 carbons in length.

The amelioration of insulin resistance in obese mice is usually accompanied by a loss of fat or body weight caused by decreased food intake[33,34], enhanced lipid oxidation and/or decreased lipogenesis[31,35,36]. The *Elovl6*$^{-/-}$ mice are unique in that their insulin resistance was reduced without amelioration of obesity or hepatosteatosis. The restoration of hepatic insulin signaling in these mice could not be explained by changes in energy balance or proinflammatory signals. These data highlight the importance of tissue fatty acid

composition in insulin sensitivity, especially the ratio of C18 to C16 fatty acids, which is controlled by Elovl6 activity. The precise molecular mechanism for this is currently unknown. Elovl6 inhibition results in the accumulation of palmitate, which is paradoxically the most potent dietary inducer of obesity and insulin resistance. Our studies show that the increase in the ratio of palmitoleate to palmitate prevents palmitate-induced *Srebf1* expression and consequently rescues palmitate-induced insulin resistance. Furthermore, our preliminary data demonstrate that overexpression of *Elovl6* leads to liver dysfunction, in addition to the induction of *Srebf1* expression and insulin resistance in cells. These results suggest that the fatty acid composition of *Elovl6*$^{-/-}$ liver, namely the high ratio of 16:1/16:0 and the reduction in C18 fatty acids, may be protective against hepatic lipotoxicity and insulin resistance in HF-HS–fed mice (**Supplementary Fig. 1b**). Feeding normal mice a diet containing a single fatty acid demonstrated that palmitate alone or stearate alone can induce insulin resistance, but oleate alone cannot (**Supplementary Fig. 5e**). *Elovl6*$^{-/-}$ mice were insulin sensitive after palmitate ingestion, with elevations in liver triglyceride and cholesterol content. Thus, the conversion of palmitate to stearate is crucial for the emergence of insulin resistance. Notably, however, *Elovl6*$^{-/-}$ mice were again resistant to the insulin resistance–inducing effects of stearate. Thus, the protective effect of *Elovl6* deficiency is not simply a result of stearate depletion, implicating that exogenous intake and endogenous production of fatty acids might have different effects on hepatic insulin sensitivity. Palmitoleate, the major final product of *de novo* fatty acid synthesis in *Elovl6* deficiency, is efficiently incorporated into triglycerides and cholesterol esters, potentially contributing to the prevention of insulin resistance[37]. These observed effects may also be related to the reported benefits of macadamia nuts rich in palmitoleate in the prevention of diabetes and cardiovascular diseases[38].

Ppara expression was reduced in *Elovl6*-deficient animals. Furthermore, Ad-Elovl6 and exogenous fatty acids administered in various 16:1/16:0 ratios regulate both *Srebf1* and *Ppara* expression in a parallel fashion, although the co-regulation of these opposite regulators of fatty acid metabolism apparently contradicts nutritional adaptation. However, the suppression of *Ppara* expression in *Elovl6*-deficient mice does not explain the restoration of insulin sensitivity in these mice. It could instead be a result of the repression of SREBP-1c. Newly synthesized fatty acids could be ligands for PPARα and hepatocyte nuclear factor-4α (ref. 30). *Elovl6* deficiency could deplete these ligands directly and/or indirectly through SREBP-1c suppression, leading to decreased activities of PPARα and hepatocyte nuclear factor-4α; it could further repress PPARα expression, as the PPARα promoter is a target of both factors (refs. 30,39,40 and T.Y. and H.S., unpublished data). Recently, we also found that knockdown of hepatic *Srebf1* leads to suppression of *Ppara* in the liver (T.Y. and H.S., unpublished data). Secondary regulation of PPARα activity could be a part of SREBP-1c/Elovl6 regulation of lipogenesis.

It has been generally noted that different long chain fatty acids have distinct effects depending upon their extent of desaturation. However, our current study suggests that the length of fatty acids is also important for energy metabolism and insulin sensitivity.

To date, *Elovl6*$^{-/-}$ mice are the only known pure metabolic model in which obesity-induced insulin resistance is mitigated through modulation of hepatic metabolism without a concurrent amelioration of obesity. It has been reported that mice deficient for inducible nitric oxide synthase, adipocyte protein-2 (also known as fatty acid binding protein-4) and mal1 (also known as fatty acid binding protein-5) also maintain insulin sensitivity despite diet-induced obesity, but not through effects on the liver[41–43]. Our model helps in understanding the mechanism by which obesity and obesity-related disorders are sometimes dissociated and implicates a new strategy for the treatment of diabetes and cardiovascular diseases through intervention of Elovl6.

METHODS

Generation of *Elovl6*$^{-/-}$ mice. *Elovl6*$^{+/-}$ founder mice created at Lexicon Genetics through the use of a gene-trapping method[44]. We identified the integration site of the targeting cassette between exon 2 and 3 and developed a PCR-based assay that distinguishes between the three possible mouse genotypes (see **Supplementary Methods** online). We crossed *Elovl6*$^{+/-}$ founder mice (50% C57BL6 albino and 50% 129SvEvBrd strains) at least six times to transfer the null mutation onto the C57BL6 genetic background. We then intercrossed heterozygotes to obtain *Elovl6*$^{+/+}$, *Elovl6* $^{+/-}$ and *Elovl6*$^{-/-}$ mice. We used only male mice for the present studies.

Animal experiments. Mice were housed in a pathogen-free barrier facility with a 12-h light/dark cycle, with free access to water and a standard chow diet. In some experiments, we fed the mice a high-carbohydrate, fat-free diet[10] or a high-fat, high-sucrose (HF-HS) diet[19]. We used age- and sex-matched littermates for each experiment, and we sacrificed mice in the early light phase in a nonfasted state. We isolated tissues immediately, weighed and kept in liquid nitrogen. We determined fat and lean mass by dual-energy X-ray absorptiometry using a PIXImus mouse densitometer (GE Medical Systems Lunar). All experiments were repeated at least three times. All animal husbandry and animal experiments were consistent with the University of Tsukuba's Regulation of Animal Experiment Committee.

Fatty acid elongation assay. We assayed microsomal fatty acid elongation activity by measuring of [2-^{14}C]malonyl-CoA incorporation into exogenous acyl-CoAs as described previously[16].

Fatty acid composition of liver. We measured the fatty acid composition by gas chromatography as described previously[45].

Metabolic measurements. We measured the concentrations of glucose, insulin, leptin, free fatty acids (FFAs), triglycerides, total cholesterol and alanine aminotransferase (ALT) in plasma and of triglycerides and total cholesterol in liver as previously described[46]. For intraperitoneal GTTs, mice were fasted overnight (for 16 h) and then injected intraperitoneally with D-glucose (20% solution; 2 g per kg body weight). For ITTs, mice in the randomly fed state were injected intraperitoneally with human regular insulin (Eli Lilly). We collected blood before injection and at different times after injection (as indicated in figures) and glucose and insulin values were determined. We determined diacylglycerol and ceramide contents in the liver lipid extracts by the diacylglycerol kinase assay as described previously[47]. We separated phosphorylated derivatives of diacylglycerol and thin-layer chromatography and visualized and quantified radioactive bands with an imaging analyzer.

***In vivo* insulin stimulation assay.** We fasted mice for 24 h and anesthetized them by injection of 30 mg/kg of pentobarbitone (Abbott Laboratories). We then opened the peritoneal cavity and injected either saline control or insulin (5 units into the inferior vena cava. After 5 min, the liver, muscle and epididymal white adipose tissue were rapidly excised and immediately frozen in liquid nitrogen. We performed immunoprecipitation and immunoblot analysis of insulin signaling molecules using tissue homogenates.

Immunoblotting and immunoprecipitation. We performed immunoblot analysis of tissue and cell lysates, membrane fractions and nuclear extracts as previously described[10,14,48]. We performed immunoprecipitation analysis of tissue lysates as previously described (ref. 14 and **Supplementary Methods**).

Total RNA preparation, northern blotting and RT-PCR analysis. We performed total RNA preparation and blot hybridization with cDNA probes as previously described[46]. We performed quantitative RT-PCR analysis as described previously (ref. 49 and **Supplementary Methods**).

Determination of fatty acid synthesis and fatty acid oxidation in mouse primary hepatocytes *in vitro*. Fatty acid synthesis and fatty acid oxidation in freshly isolated hepatocytes were measured as previously described[50].

Preparation of recombinant adenovirus and adenovirus treatment. We subcloned *Elovl6*-specific RNA interference (RNAi) constructs into the U6 entry vector (Invitrogen) using a primer specific for the *Elovl6* coding sequence, 5′-GCGAGCCAAGTTTGAACTTCAGA-3′, and generated the recombinant adenoviral plasmid by homologous recombination with the pAd promoterless vector (Invitrogen). We subcloned mouse *Elovl6*-coding cDNA into the pENTR/D-TOPO vector (Invitrogen) and generated recombinant adenoviral plasmid by homologous recombination with pAd/CMV/V5-DEST vector (Invitrogen). We produced recombinant adenovirus in HEK293 cells and purified them as previously described[14,48]. We intravenously injected mice with adenoviruses expressing LacZ RNAi or Elovl6 RNAi at a dose of 1×10^9 PFU and adenoviruses expressing GFP or Elovl6 at a dose of 1×10^8 PFU. Cells were infected with adenoviruses expressing GFP or Elovl6 at a multiplicity of infection of 100 for 16 h.

Culture of Hepa1c1c7 cells. Mouse hepatoma Hepa1c1c7 cells were cultured in MEMα supplemented with 10% FBS and 1% penicillin/streptomycin. For insulin-signaling analysis, we changed cells into serum-free medium 4 h before the experiment and then treated them with or without insulin (100 nM, 10 min). Cells were treated with fatty acids as described previously[49].

Statistical analyses. Data are expressed as means ± s.e.m. Differences between two groups were assessed using the unpaired two-tailed Student's *t*-test. Data sets involving more than two groups were assessed by ANOVA. Glucose and insulin tolerance tests were analyzed by repeated-measures ANOVA with Statview Software (BrainPower).

Note: Supplementary information is available on the Nature Medicine website.

ACKNOWLEDGMENTS

We thank T. Ide and H. Daitoku for technical help and/or useful comments. This work was supported by grants-in-aid from the Ministry of Science, Education, Culture and Technology of Japan; a grant for the Japan Foundation for Applied Enzymology; and a grant from The Naito Foundation.

AUTHOR CONTRIBUTIONS

T. Matsuzaka carried out most of the experiments, data analysis and prepared the figures with significant help from M.I., S.O., N. Ishigaki, H.I., Y.I. and T. Karasawa. H. Shimano developed the idea for and supervised the study, designed protocols, developed collaborations and wrote the manuscript. N. Yahagi contributed to many *in vivo* experiments and to training T. Matsuzaka in experimental techniques. T. Kato carried out measurements of fatty acid composition and assisted with hepatocyte isolations, fatty acid treatment to the cell and mice and adenoviral experiments. A.A. assisted with the *in vivo* adenoviral experiments. T.Y. assisted with PKCε analysis and cell-line experiments. N. Inoue assisted with ELISA measurements and developed the DXA protocols for analyzing fat. S.K. assisted with RT-PCR analysis. T. Matsui contributed to primary myotube culture and the 2-DG uptake assay. M.S. and K.O. participated in the experimental design and in training T. Matsuzaka in experimental techniques. A.H.H. reviewed the manuscript. Y.N. contributed to immunoblot analysis of insulin signaling, adenoviral work and discussion of the results. A.T. contributed to GTT, ITT, HF-HS diet–feeding to the mice and discussion of the results. H. Suzuki, S.Y., H. Sone, H.T. and J.O. contributed to experimental design, data analysis, interpretation and presentation. N. Yamada supervised the study, contributed crucial ideas to the project and reviewed the manuscript.

Published online at http://www.nature.com/naturemedicine
Reprints and permissions information is available online at http://npg.nature.com/reprintsandpermissions

1. Riccardi, G., Giacco, R. & Rivellese, A.A. Dietary fat, insulin sensitivity and the metabolic syndrome. *Clin. Nutr.* **23**, 447–456 (2004).
2. Unger, R.H. Minireview: weapons of lean body mass destruction: the role of ectopic lipids in the metabolic syndrome. *Endocrinology* **144**, 5159–5165 (2003).
3. Cai, D. *et al.* Local and systemic insulin resistance resulting from hepatic activation of IKKβ and NFβB. *Nat. Med.* **11**, 183–190 (2005).
4. Arkan, M.C. *et al.* IKK-beta links inflammation to obesity-induced insulin resistance. *Nat. Med.* **11**, 191–198 (2005).
5. Nakatani, Y. *et al.* Modulation of the JNK pathway in liver affects insulin resistance status. *J. Biol. Chem.* **279**, 45803–45809 (2004).
6. Ozcan, U. *et al.* Endoplasmic reticulum stress links obesity, insulin action, and type 2 diabetes. *Science* **306**, 457–461 (2004).
7. Howard, J.K. *et al.* Enhanced leptin sensitivity and attenuation of diet-induced obesity in mice with haploinsufficiency of Socs3. *Nat. Med.* **10**, 734–738 (2004).
8. Inoue, H. *et al.* Role of hepatic STAT3 in brain-insulin action on hepatic glucose production. *Cell Metab.* **3**, 267–275 (2006).
9. Torisu, T. *et al.* The dual function of hepatic SOCS3 in insulin resistance *in vivo*. *Genes Cells* **12**, 143–154 (2007).
10. Shimano, H. *et al.* Sterol regulatory element-binding protein-1 as a key transcription factor for nutritional induction of lipogenic enzyme genes. *J. Biol. Chem.* **274**, 35832–35839 (1999).
11. Shimano, H. Sterol regulatory element-binding proteins (SREBPs): transcriptional regulators of lipid synthetic genes. *Prog. Lipid Res.* **40**, 439–452 (2001).
12. Horton, J.D. *et al.* Combined analysis of oligonucleotide microarray data from transgenic and knockout mice identifies direct SREBP target genes. *Proc. Natl. Acad. Sci. USA* **100**, 12027–12032 (2003).
13. Lin, J. *et al.* Hyperlipidemic effects of dietary saturated fats mediated through PGC-1beta coactivation of SREBP. *Cell* **120**, 261–273 (2005).
14. Ide, T. *et al.* SREBPs suppress IRS-2-mediated insulin signalling in the liver. *Nat. Cell Biol.* **6**, 351–357 (2004).
15. Moon, Y.A., Shah, N.A., Mohapatra, S., Warrington, J.A. & Horton, J.D. Identification of a mammalian long chain fatty acyl elongase regulated by sterol regulatory element-binding proteins. *J. Biol. Chem.* **276**, 45358–45366 (2001).
16. Matsuzaka, T. *et al.* Cloning and characterization of a mammalian fatty acyl-CoA elongase as a lipogenic enzyme regulated by SREBPs. *J. Lipid Res.* **43**, 911–920 (2002).
17. Leonard, A.E., Pereira, S.L., Sprecher, H. & Huang, Y.S. Elongation of long-chain fatty acids. *Prog. Lipid Res.* **43**, 36–54 (2004).
18. Wang, Y. *et al.* Regulation of hepatic fatty acid elongase and desaturase expression in diabetes and obesity. *J. Lipid Res.* **47**, 2028–2041 (2006).
19. Maeda, N. *et al.* Diet-induced insulin resistance in mice lacking adiponectin/ACRP30. *Nat. Med.* **8**, 731–737 (2002).
20. Weisberg, S.P. *et al.* Obesity is associated with macrophage accumulation in adipose tissue. *J. Clin. Invest.* **112**, 1796–1808 (2003).
21. Xu, H. *et al.* Chronic inflammation in fat plays a crucial role in the development of obesity-related insulin resistance. *J. Clin. Invest.* **112**, 1821–1830 (2003).
22. Nakae, J., Kitamura, T., Silver, D.L. & Accili, D. The forkhead transcription factor Foxo1 (Fkhr) confers insulin sensitivity onto glucose-6-phosphatase expression. *J. Clin. Invest.* **108**, 1359–1367 (2001).
23. Wolfrum, C., Asilmaz, E., Luca, E., Friedman, J.M. & Stoffel, M. Foxa2 regulates lipid metabolism and ketogenesis in the liver during fasting and in diabetes. *Nature* **432**, 1027–1032 (2004).
24. Zhou, G. *et al.* Role of AMP-activated protein kinase in mechanism of metformin action. *J. Clin. Invest.* **108**, 1167–1174 (2001).
25. Samuel, V.T. *et al.* Mechanism of hepatic insulin resistance in non-alcoholic fatty liver disease. *J. Biol. Chem.* **279**, 32345–32353 (2004).
26. Yu, C. *et al.* Mechanism by which fatty acids inhibit insulin activation of insulin receptor substrate-1 (IRS-1)-associated phosphatidylinositol 3-kinase activity in muscle. *J. Biol. Chem.* **277**, 50230–50236 (2002).
27. Holland, W.L. *et al.* Inhibition of ceramide synthesis ameliorates glucocorticoid-, saturated-fat-, and obesity-induced insulin resistance. *Cell Metab.* **5**, 167–179 (2007).
28. Samuel, V.T. *et al.* Inhibition of protein kinase Cepsilon prevents hepatic insulin resistance in nonalcoholic fatty liver disease. *J. Clin. Invest.* **117**, 739–745 (2007).
29. Friedman, J.M. Obesity in the new millennium. *Nature* **404**, 632–634 (2000).
30. Chakravarthy, M.V. *et al.* "New" hepatic fat activates PPARalpha to maintain glucose, lipid, and cholesterol homeostasis. *Cell Metab.* **1**, 309–322 (2005).
31. Ntambi, J.M. *et al.* Loss of stearoyl-CoA desaturase-1 function protects mice against adiposity. *Proc. Natl. Acad. Sci. USA* **99**, 11482–11486 (2002).
32. Dobrzyn, P. *et al.* Stearoyl-CoA desaturase 1 deficiency increases fatty acid oxidation by activating AMP-activated protein kinase in liver. *Proc. Natl. Acad. Sci. USA* **101**, 6409–6414 (2004).
33. Shimada, M., Tritos, N.A., Lowell, B.B., Flier, J.S. & Maratos-Flier, E. Mice lacking melanin-concentrating hormone are hypophagic and lean. *Nature* **396**, 670–674 (1998).
34. Loftus, T.M. *et al.* Reduced food intake and body weight in mice treated with fatty acid synthase inhibitors. *Science* **288**, 2379–2381 (2000).
35. Elchebly, M. *et al.* Increased insulin sensitivity and obesity resistance in mice lacking the protein tyrosine phosphatase-1B gene. *Science* **283**, 1544–1548 (1999).
36. Abu-Elheiga, L., Matzuk, M.M., Abo-Hashema, K.A. & Wakil, S.J. Continuous fatty acid oxidation and reduced fat storage in mice lacking acetyl-CoA carboxylase 2. *Science* **291**, 2613–2616 (2001).
37. Neumann-Haefelin, C. *et al.* Muscle-type specific intramyocellular and hepatic lipid metabolism during starvation in wistar rats. *Diabetes* **53**, 528–534 (2004).
38. Hiraoka-Yamamoto, J. *et al.* Serum lipid effects of a monounsaturated (palmitoleic) fatty acid–rich diet based on macadamia nuts in healthy, young Japanese women. *Clin. Exp. Pharmacol. Physiol.* **31** Suppl 2, S37–S38 (2004).
39. Kliewer, S.A. *et al.* Fatty acids and eicosanoids regulate gene expression through direct interactions with peroxisome proliferator-activated receptors alpha and gamma. *Proc. Natl. Acad. Sci. USA* **94**, 4318–4323 (1997).
40. Wisely, G.B. *et al.* Hepatocyte nuclear factor 4 is a transcription factor that constitutively binds fatty acids. *Structure* **10**, 1225–1234 (2002).
41. Perreault, M. & Marette, A. Targeted disruption of inducible nitric oxide synthase protects against obesity-linked insulin resistance in muscle. *Nat. Med.* **7**, 1138–1143 (2001).
42. Hotamisligil, G.S. *et al.* Uncoupling of obesity from insulin resistance through a targeted mutation in aP2, the adipocyte fatty acid binding protein. *Science* **274**, 1377–1379 (1996).

43. Maeda, K. *et al.* Role of the fatty acid binding protein mal1 in obesity and insulin resistance. *Diabetes* **52**, 300–307 (2003).
44. Zambrowicz, B.P. *et al.* Disruption and sequence identification of 2,000 genes in mouse embryonic stem cells. *Nature* **392**, 608–611 (1998).
45. Sekiya, M. *et al.* Polyunsaturated fatty acids ameliorate hepatic steatosis in obese mice by SREBP-1 suppression. *Hepatology* **38**, 1529–1539 (2003).
46. Matsuzaka, T. *et al.* Insulin-independent induction of sterol regulatory element-binding protein-1c expression in the livers of streptozotocin-treated mice. *Diabetes* **53**, 560–569 (2004).
47. Turinsky, J., O'Sullivan, D.M. & Bayly, B.P. 1,2-Diacylglycerol and ceramide levels in insulin-resistant tissues of the rat *in vivo*. *J. Biol. Chem.* **265**, 16880–16885 (1990).
48. Nakagawa, Y. *et al.* TFE3 transcriptionally activates hepatic IRS-2, participates in insulin signaling and ameliorates diabetes. *Nat. Med.* **12**, 107–113 (2006).
49. Kato, T. *et al.* Granuphilin is activated by SREBP-1c and involved in impaired insulin secretion in diabetic mice. *Cell Metab.* **4**, 143–154 (2006).
50. Jiang, G. *et al.* Prevention of obesity in mice by antisense oligonucleotide inhibitors of stearoyl-CoA desaturase-1. *J. Clin. Invest.* **115**, 1030–1038 (2005).

Original Article

Pitavastatin Decreases Plasma Preβ1-HDL Concentration and Might Promote its Disappearance Rate in Hypercholesterolemic Patients

Mikihiko Kawano[1], Shoichiro Nagasaka[2], Hiroaki Yagyu[2], and Shun Ishibashi[2]

[1]Department of Comprehensive Medicine, Jichi Medical University, Omiya Medical Center
[2]Division of Endocrinology and Metabolism, Department of Medicine, Jichi Medical University

Aim: Preβ1-HDL is involved in the initial step of cholesterol efflux from peripheral cells and plays an important role in reverse cholesterol transport. We studied the effect of pitavastatin on the HDL subfraction profile, preβ1-HDL concentration and its disappearance rate.
Methods: Twenty-nine hypercholesterolemic patients were treated with pitavastatin at 2 mg/day for 4 weeks, and plasma levels of total cholesterol (TC), triglyceride, HDL-cholesterol (C), HDL_2-C, HDL_3-C, preβ1-HDL, LCAT activity, and CETP mass were assayed. The preβ1-HDL disappearance rate was determined as the difference in preβ1-HDL concentration before and after incubation at 37℃ for 90 min divided by the pre-incubation preβ1-HDL concentration.
Results: Pitavastatin led to significant decreases in TC by 26.9% and LDL-C by 39.8%. HDL-C and HDL_2-C increased significantly by 6.0% and 9.0%, respectively, but there was no significant change in HDL_3-C. Preβ1-HDL concentration significantly decreased (−8.7%; $p<0.05$); however, its disappearance rate significantly increased (13.0%; $p<0.05$). There were significant decreases in both LCAT activity and CETP mass.
Conclusion: Although pitavastatin decreased plasma preβ1-HDL concentration, it increased the preβ1-HDL disappearance rate. These data suggest that pitavastatin might promote the early step of reverse cholesterol transport.

J Atheroscler Thromb, 2008; 15:41-46.

Key words; Statin, HDL subfraction, preβ1-HDL, LCAT

Introduction

High-density lipoprotein (HDL) is the only anti-atherosclerotic lipoprotein in plasma and its clinical significance has attracted attention[1]. One important mechanism of the anti-atherosclerotic effect of HDL is its role in reverse cholesterol transport (RCT)[2]. This effect is supposed to be prominent in patients with high plasma levels of HDL-cholesterol (HDL-C). Many epidemiological studies have demonstrated that HDL-C is a negative risk factor for coronary artery disease[3-5]; however, there are also reports that the plasma HDL-C concentration does not always reflect the magnitude of its anti-atherosclerotic effect, and this issue remains the subject of debate[6].

Preβ1-HDL, a subclass of HDL migrating to the preβ position on agarose gel electrophoresis, plays an important role in the initial step of RCT[7]. In one pathway, called the specific pathway, preβ1-HDL interacts with cell membranes and takes up cholesterol via ATP-binding cassette (ABC) A1 expressed on the cell surface. Preβ1-HDL conversion to α-HDL is one of the critical steps in this specific RCT and is mediated by lecithin: cholesterol acyltransferase (LCAT)[8]. Although the clinical significance of plasma preβ1-HDL concentration and its conversion reaction is not completely clear, accumulating evidence suggests that impaired conversion of preβ1-HDL, resulting in high plasma preβ1-HDL concentration, is involved in the initiation and progression of atherosclerosis.

HMG-CoA reductase inhibitors (statins) are

Address for correspondence: Mikihiko Kawano, Department of Comprehensive Medicine, Jichi Medical University, Omiya Medical Center, 1-847 Amanuma-cho, Omiya-ku, Saitama-shi, Saitama-ken, 330-8503, Japan.
E-mail: mkkawano@jichi.ac.jp
Received: July 23, 2007
Accepted for publication: November 5, 2007

widely used to treat hypercholesterolemia and have proved the usefulness of primary and secondary prevention for cardiovascular disease. The anti-atherosclerotic effect of statins on plasma lipoproteins can be explained largely by the reduction of LDL-C levels[9, 10]; the effects are thought to involve the elevation in HDL-C[11]. The effects of statins on plasma lipoproteins in Japanese hyperlipidemic patients have been described[12, 13]; however, the mechanisms are not completely clear. Although there are several reports of the effects of statins on the HDL subfraction profile and plasma preβ1-HDL concentration[14, 15], there have been no studies of their effects on the disappearance of preβ1-HDL.

In this study, we assessed the effects of pitavastatin on the HDL subfraction profile and the disappearance rate of preβ1-HDL in patients with hypercholesterolemia. We also assessed changes in LCAT activity and the cholesteryl ester transfer protein (CETP) mass, which play important roles in HDL metabolism.

Materials and Methods

The institutional ethics committee of Jichi Medical University approved the conduct of this study from January to December, 2004. The principal investigator or sub-investigator provided adequate explanation to the subjects concerning this study, and the subjects consented to participate and gave written consent.

Twenty-nine subjects (15 men, 14 women; mean age: 57.31 ± 11.0 years (29 – 74)) with hypercholesterolemia were recruited. Eleven subjects had type 2 diabetes (7 men, 4 women). The inclusion criteria were: patients whose physician had determined that pitavastatin was needed, patients with type IIa or IIb hyperlipidemia who were adult men or post-menopausal women with total cholesterol (TC) of 220 mg/dL or greater, triglyceride (TG) of 400 mg/dL or less, and patients not receiving other HMG-CoA reductase inhibitors. The exclusions were: patients with serious hepatic or renal dysfunction, poorly controlled diabetes or severe hypertension, hypothyroidism, patients on cyclosporin, patients with recent myocardial infarction or cerebrovascular accident (within 3 months of the event), patients with heart failure, patients with drug or alcohol abuse, patients with a history of drug hypersensitivity or serious adverse drug reactions.

The subjects were treated with pitavastatin 2 mg/day for 4 weeks. During the study, co-administration of drugs that may affect serum lipids (drugs for hyperlipidemia other than the study drug, drugs for insulin resistance, various hormonal agents, anti-psychotic agents, tricyclic antidepressants, cholagogue drugs, anti-obesity drugs or appetite-stimulating drugs, levothyroxin, immunosuppressive agents) was prohibited. Concurrent administration of other drugs was permitted. Whenever possible, the type and dose were not changed during the study. The subjects were instructed to maintain their normal daily activities and diet during the study without any change. On the day prior to blood drawing, excessive eating and drinking, including alcohol after 9 pm, were prohibited. On the day of blood drawing, the subjects fasted prior to the blood drawing, although water was permitted. At week 0 and 4, a fasting blood sample was collected into an EDTA containing a glass tube precooled with ice-water. Plasma was separated by centrifugation at 0℃ and further analysis was performed immediately.

Lipoprotein Assay

TC, TG, and HDL-C were measured by automated enzymatic assays, LDL-C was calculated by the Friedewald formula (LDL-C = (TC – HDL-C) – TG/5)[16]. HDL_2-C and HDL_3-C were measured by automated enzymatic assay after ultracentrifugation. Preβ1-HDL was measured by a sandwich enzyme immunoassay using an anti-preβ1-HDL antibody, reported by Miyazaki *et al.* (Mab55201, Daiichi Pure Chemicals Co., Ltd., Tokyo)[17].

Determination of Preβ1-HDL Disappearance Rate

To determine the disappearance rate of preβ1-HDL, we incubated plasma at 37℃ for 90 min and measured the preβ1-HDL concentration before and after incubation. The disappearance rate was defined as the difference in preβ1-HDL concentration before and after incubation divided by the pre-incubation preβ1-HDL concentration: {disappearance rate = [(preβ1-HDL concentration before incubation) – (preβ1-HDL concentration after incubation at 37℃ for 90 min.)] / (preβ1-HDL concentration before incubation)}, reported by Fielding *et al.*[18].

Enzyme Activity Assays

LCAT activity was determined by the method of Nagasaki *et al.*[19] using dipalmitoyl lecithin as the substrate, and CETP mass was determined by an ELISA assay (CETP ELIZA-DAIICHI, Daiichi Pure Chemicals Co., Ltd., Tokyo).

Statistical Analysis

Each parameter was analyzed using the one-sample *t*-test. The correlation between variables was assessed using Pearson's correlation coefficient test. The significance level was 5% (two-tailed), and data are expressed as the mean ± standard deviation.

Table 1. Effects of pitavastatin on plasma lipids in 29 hypercholesterolemic patients

	before treatment	after treatment	% change
TC (mg/dL)	277±63	200±38***	−26.9
TG (mg/dL)	136±78	126±74	−2.7
LDL-C (mg/dL)	195±62	117±39***	−39.8
HDL-C (mg/dL)	54.3±14.6	57.4±16.1**	+6.0

***$p<0.001$, **$p<0.01$

Table 2. Effects of pitavastatin on HDL subfraction, disappearance rate of preβ1-HDL, LCAT activity and CETP mass

	normal range	before treatment	after treatment	% change
HDL_2-C (mg/dL)	16.0-73.0	35.4±13.7	38.6±16.1***	+9.0
HDL_3-C (mg/dL)	13.0-25.0	19.5±3.0	19.5±3.0	+0.9
Preβ1HDL (μg/dL)	15.0-30.0[28]	14.9±9.1	12.3±6.0*	−8.7
Disappearance rate of Preβ1-HDL (%)		66.8±16.0	71.9±10.1*	+13.0
LCAT activity (nmol/mL/hr/37℃)	53.3-108.2	125±24	103±21***	−16.9
CETP mass (μg/mL)	0.8-3.0	2.0±0.3	1.8±0.4**	−7.6

***$p<0.001$, **$p<0.01$, *$p<0.05$

Results

Changes in Plasma Lipids and Lipoproteins

After treatment with pitavastatin of 2 mg/day for 4 weeks, TC decreased by −26.9% ($p<0.001$) and LDL-C by −39.8% ($p<0.001$). HDL-C increased significantly by +6.0% ($p<0.01$). On the other hand, TG changed by −2.7%, which was not significant (**Table 1**).

Changes in HDL Subfractions, Preβ1-HDL Concentrations and its Conversion Rate, LCAT Activity, and CETP Mass

HDL_2-C increased significantly by +9.0% ($p<0.001$), while HDL_3-C increased by +0.9%, which was not significant (**Table 2**). Preβ1-HDL concentration decreased significantly by −8.7% ($p<0.05$), while the preβ1-HDL conversion rate increased significantly by +13.0% ($p<0.05$) (**Table 2**). LCAT activity decreased significantly by −16.9% ($p<0.05$). CETP decreased significantly by −7.6% ($p<0.01$). The changes in LCAT activity showed a significant positive correlation with the changes in LDL-C ($r=0.44$; $p<0.05$) (**Fig. 1**).

Correlation between LCAT Activity and Preβ1-HDL Disappearance Rate

LCAT activity did not correlate with the preβ1-HDL concentration (data not shown), although there was a significant positive correlation between LCAT activity and the preβ1-HDL disappearance rate. There was no change in the positive correlation with the same slope before or after treatment, but the preβ1-HDL disappearance rate was higher after pitavastatin treatment (**Fig. 2**).

Discussion

To assess the effects of pitavastatin on the RCT, plasma lipids, HDL subfractions, the disappearance rate of preβ1-HDL, LCAT activity, and CETP mass were assayed. The results indicate that pitavastatin decreases the plasma preβ1-HDL concentration and might promote the disappearance of preβ1-HDL.

In this study, pitavastatin significantly increased HDL-C by 6.0%. In the HDL subfractions, there was a significant increase in HDL_2-C by 9.0% but essentially no change in HDL_3-C. The mechanism of the pitavastatin-induced increase of HDL-C has been reported in *in vitro* studies to be the promotion of apoprotein-AI production from HepG2 cells mediated via the activation of peroxisome proliferator-activated receptor α (PPARα)[20, 21]. Many studies, but not all, have shown that HDL with a larger particle size (HDL_2) has relatively potent anti-atherosclerotic effects[22, 23]. Increased HDL_2 might promote non-specific cholesterol efflux from the cells[24].

In regard to the clinical significance of the plasma preβ1-HDL concentration and its disappearance, supposing conversion to α-HDL, accumulating evidence suggests that impaired conversion of preβ1-HDL resulting in high plasma preβ1-HDL concen-

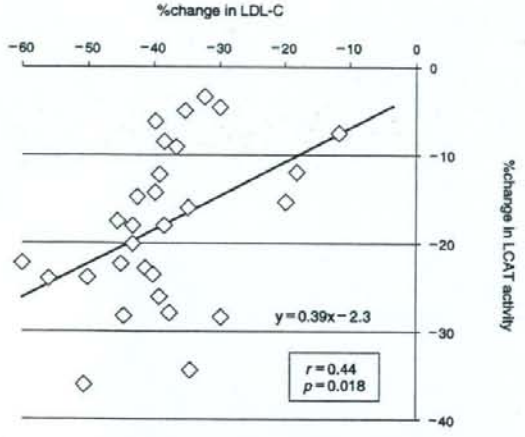

Fig. 1. The relation between the changes in LDL-C and in LCAT activity after 4 weeks of treatment in 29 hyperlipidemia patients was investigated by Pearson's correlation coefficient test.

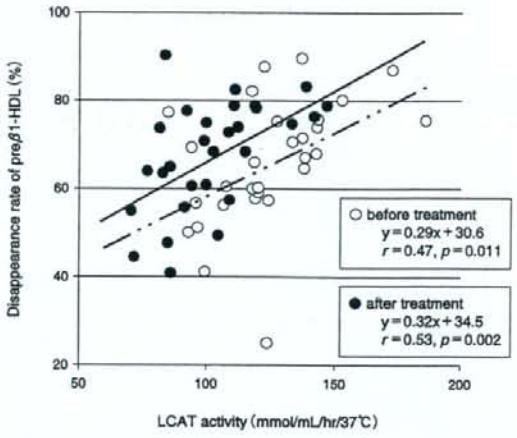

Fig. 2. The relation between LCAT activity and conversion rate of preβ1-HDL to α-HDL before (open circles) and after (closed circles) pitavastatin treatment was investigated by Pearson's correlation coefficient test.

tration is involved in the initiation and progression of atherosclerosis[25-27]. In this study, pitavastatin also significantly decreased plasma preβ1-HDL concentration, but significantly increased the disappearance rate of preβ1-HDL. Miida *et al.*[25] have reported that the preβ1-HDL conversion rate is a major determinant of plasma preβ1-HDL concentration. In fact, patients who have an impaired conversion rate of preβ1-HDL have high plasma preβ1-HDL concentration[25, 27]. Decreased plasma preβ1-HDL concentration by pitavastatin in this study may be thought to be primarily due to the increased disappearance rate. Based on these observations, pitavastatin is proposed to act as an antiatherosclerotic.

Asztalos *et al.*[14] have reported the effects of five different statins, excluding pitavastatin, on HDL subpopulation profiles analyzed by 2-dimensional electrophoresis. Preβ1-HDL concentrations after 4-week treatment with each statin were consistently increased, different from our study, although the extent varied. These differences from our study be a result of the HDL-subpopulation analytical method, subjects who were all coronary heart disease patients, or the dosage of statins, although the precise causes are not clear. To further confirm this effect of pitavastatin, future work is needed using a larger sample size with a comparative study design.

LCAT is an important enzyme involved in the maturation of preβ1-HDL to α-HDL[28]. Cell-derived free cholesterol on preβ1-HDL is converted to cholesterol ester by LCAT and stored in the core of HDL particles[8], and simultaneously smaller discoidal preβ1-HDL converts to larger spherical α-HDL. In this study, pitavastatin decreased LCAT activity and plasma preβ1-HDL concentration, but increased its disappearance rate, in contrast to previous reports; however, LCAT exists in two forms, α-LCAT present in the high-density fraction ($1.121 < d. < 1.25$) and β-LCAT present in the low-density fraction ($1.019 < d. < 1.063$), and it is known that α-LCAT is important for the maturation of preβ1-HDL to α-HDL[29, 30]. The LCAT activity in this study was the sum of α- and β-LCAT activities[19], because it is impossible to measure α- or β-LCAT activity individually. There was a positive correlation between the decrease in LDL-C and the decrease in LCAT activity in this study (**Fig. 1**). It is supposed that the decrease in LCAT activity by pitavastatin might be due to a decrease in β-LCAT activity, not α-LCAT activity.

This study also demonstrated a significant positive correlation between LCAT activity and the preβ1-HDL disappearance rate. Although there was no change in the positive correlation with the same slope before or after treatment, the preβ1-HDL disappearance rate was higher after pitavastatin treatment (**Fig. 2**). The cause is still unclear and needs to be studied in the future, but it is suggested that pitavastatin might promote preβ1-HDL disappearance by a mechanism independent of LCAT activity.

There have been several reports that statins de-

crease CETP[31], and our data also showed a decrease in the CETP mass. CETP is involved in the production of preβ1-HDL from α-HDL[32], and a positive correlation has been reported between CETP and preβ1-HDL[32, 33], thus, our data are in agreement. Since the magnitude of the CETP decrease is small, it is unclear whether the pitavastatin-induced decrease in CETP is truly involved in the decrease in preβ1-HDL.

It has been demonstrated that the formation and metabolism of preβ1-HDL was influenced by hepatic lipase (HL) activity and phospholipid transfer protein (PLTP) activity[34]. As a limitation of our study, we did not evaluate the effects of these factors on preβ1-HDL concentration and its disappearance rate, which were included in the conversion pathway of preβ1-HDL to α-HDL and other metabolic pathways of preβ1-HDL.

In conclusion, our data showed that the HMG-CoA reductase inhibitor pitavastatin: 1) markedly decreased TC and LDL-C and significantly increased HDL-C and HDL2-C, 2) decreased plasma preβ1-HDL concentration but promoted its disappearance, 3) and decreased plasma LCAT activity, which correlated positively with the decrease in LDL-C. These data indicate that pitavastatin, in addition to decreasing LDL-C, might also exert a potent anti-atherosclerotic effect by improving the HDL subfraction profile and promoting the early step of RCT; however, further work is required.

Acknowledgement

The authors thank Mr. Takashi Nakamura (Medical Affairs Department, Kowa Co. Ltd., Tokyo, Japan) for important suggestions.

References

1) Gordon DJ and Rifkind BM: High-density lipoprotein-the clinical implications of recent studies. New Engl J Med, 1989; 321:1311-1316
2) Hill SA and McQueen MJ: Reverse cholesterol transport-a review of the process and its clinical implications. Clin Biochem, 1997; 30:517-525
3) Castelli WP: Epidemiology of coronary heart disease: the Framingham study. Am J Med, 1984; 76:4-12
4) Miller NE, Forde OH, Thelle DS, and Mjos OD: The Tromso Heart Study. High-density lipoprotein and coronary heart disease: a prospective case-control study. Lancet, 1977; 1:965-968
5) Gordon DJ, Probstfield JL, Garrison RJ, Neaton JD, Castelli WP, Knoke JD, Jacobs DR, Bangdiwala S Jr., and Tyroler HA: High-density lipoprotein cholesterol and cardiovascular disease. Four prospective American studies. Circulation, 1989; 79:8-15
6) Eckardstein A and Assmann G: Prevention of coronary heart disease by raising high-density lipoprotein cholesterol? Curr Opin Lipidol, 2000; 11:627-637
7) Fielding CJ and Fielding PE: Molecular physiology of reverse cholesterol transfer. J Lipid Res, 1995; 36:211-228
8) Miida T, Kawano M, Fielding CJ, and Fielding PE: Regulation of the concentration of preβ high-density lipoprotein in normal plasma by cell membranes and lecithin-cholesterol acyltransferase activity. Biochemistry, 1992; 31:11112-11117
9) Gould GR, Rossouw JE, Santanello NC, Heyse JF, and Furberg CD: Cholesterol reduction yields clinical benefit: impact of statin trials. Circulation, 1998; 97:946-952
10) Pedersen TR: Pro and Con: Low-density lipoprotein cholesterol lowering is and will be the key to the future of lipid management. Am J Cardiol, 2001; 87 (5A):8B-12B
11) Schaefer JR, Schweer H, Ikewaki K, Stracke H, Seyberth HJ, Kaffarnik H, Maisch B, and Steinmetz A: Metabolic basis of high density lipoproteins and apolipoprotein A-I increase by HMG-CoA reductase inhibition in healthy subjects and a patients with coronary artery disease. Atherosclerosis, 1999; 144:177-184
12) Endo K, Miyashita Y, Saiki A, Oyama T, Koide N, Ozaki H, Otsuka M, Ito Y, and Shirai K: Atorvastatin and pitavastatin elevated pre-heparin lipoprotein lipase mass of type 2 diabetes with hypercholesterolemia. J Atheroscler Thromb, 2004; 11:341-347
13) Yoshitomi Y, Ishii T, Kaneki M, Tsujibayashi T, Sakurai S, Nagakura C, and Miyauchi A: Efficacy of a low dose of pitavastatin compared with atorvastatin in primary hyperlipidemia: results of a 12-week, open label study. J Atheroscler Thromb, 2006; 13:108-113
14) Asztalos BF, Horvath KV, McNamara JR, Roheim PS, Rubinstein JJ, and Schaefer EJ: Comparing the effects of five different statins on the HDL subpopulation profiles of coronary heart disease patients. Atherosclerosis, 2002; 164:361-369
15) Asztalos BF, Horvath KV, McNamara JR, Roheim PS, Rubinstein JJ, and Schaefer EJ: Effects of atorvastatin on the HDL subpopulation profile of coronary heart disease patients. J Lipid Res, 2002; 43:1701-1707
16) Friedewald WT, Levy RI, and Fredrickson DS: Estimation of the concentration of low-density lipoprotein cholesterol in plasma, without use of the preparative ultracentrifuge. Clin Chem, 1972; 18:499-502
17) Miyazaki O, Kobayashi J, Fukamachi I, Miida T, Bujo H, and Saito Y: A new sandwich enzyme immunoassay for measurement of plasma pre-β1-HDL levels. J Lipid Res, 2000; 41:2083-2088
18) Fielding CJ and Fielding PE: Regulation of human lecithin: cholesterol acyltransferase activity by lipoprotein acceptor cholesteryl ester content. J Biol Chem, 1981; 256:2102-2104
19) Nagasaki T and Akanuma Y: A new colorimetric method for the determination of plasma lecithin-cholesterol acyltransferase activity. Clin Chim Acta, 1977; 75:371-375
20) Martin G, Duez H, Blanquart C, Berezowski V, Poulain P, Fruchart JC, Najib-Fruchart J, Glineur C, and Staels B: Statin-induced inhibition of the Rho-signaling pathway activates PPARα and induces HDL apoA-I. J Clin Invest, 2001; 107:1423-1432

21) Maejima T, Yamazaki H, Aoki T, Tamaki T, Sato F, Kitahara M, and Saito Y: Effect of pitavastatin on apolipoprotein A-I production in HepG2 cell. Biochem Biophys Res Commun, 2004; 324:835-839
22) Sweetnam PM, Bolton CH, Yarnel IW, Bainton D, Baker IA, Elwood PC, and Miller NE: Association of HDL_2 and HDL_3 cholesterol subfractions with the development of ischemic heart disease in British men. Circulation, 1994; 90:769-774
23) Campos H, Roederer GO, Lussier-Cacan S, Davignon J, and Krauss RM: Predominance of large LDL and reduced HDL_{-2} cholesterol in normolipidemic men with coronary artery disease. Arterioscl Thromb Vasc Biol, 1995; 15:1043-1048
24) McLean LR and Phillips MC: Mechanism of cholesterol and phosphatidylcholine exchange or transfer between unilamellar vesicles. Biochemistry, 1981; 20:2893-2900
25) Miida T, Nakamura Y, Inano K, Matsuto T, Yamaguchi T, Tsuda T, and Okada M: Preβ1-high-density lipoprotein increases in coronary artery disease. Clin Chem, 1996; 42:1992-1995
26) Asztalos BF, Roheim PS, Milani RL, Lefevre M, McNamara JR, Horvath KV, and Schaefer EJ: Distribution of apoA-I-containing HDL subpopulations in patients with coronary heart disease. Arterioscler Thromb Vasc Biol, 2000; 20:2670-2676
27) Miida T, Miyazaki O, Hanyu O, Nakamura Y, Hirayama S, Narita I, Gejyo F, Ei I, Tasaki K, Kohoda T, Yata S, Fukamachi I, and Okada M: LCAT-dependent conversion of preβ1-HDL into α-migrating HDL is severely delayed in hemodialysis patients. J Am Soc Nephrol, 2003; 14:732-738
28) Miida T, Obayashi K, Seino U, Zhu Y, Ito T, Kosuge K, Hirayama S, Hanyu O, Nakamura Y, Yamaguchi T, Tsuda T, Saito Y, Miyazaki O, Nakamura Y, and Okada M: LCAT-dependent conversion rate is a determinant of plasma preβ-HDL in healthy Japanese. Clin Chim Acta, 2004; 350:107-114
29) Francone OL, Gurakar A, and Fielding CJ: Distribution and functions of lecithin: cholesterol acyltransferase and cholesteryl ester transfer protein in plasma lipoproteins. Evidence for a functional unit containing these activities together with apolipoproteins A-I and D that catalyzes the esterification and transfer of cell-derived cholesterol. J Biol Chem, 1989; 264:7066-7072
30) Vanloo B, Peelman F, Deschuymere K, Taveirne J, Verhee A, Gouyette C, Labeur C, Vandekerckhove J, Tavernier J, and Rosseneu M: Relationship between structure and biochemical phenotype of lecithine: cholesterol acyltransferase (LCAT) mutants causing fish-eye disease. J Lipid Res, 2000; 41:752-761
31) Homma Y, Ozawa H, Kobayashi T, Yamaguchi H, Sakane H, and Nakamura H: Effects of simvastatin on plasma lipoprotein subfractions, cholesterol esterification rate, and cholesteryl ester transfer protein in type II hyperlipoproteinemia. Atherosclerosis, 1995; 114:223-234
32) Francone OL, Royer L, and Haghpassand M: Increased prebeta-HDL levels, cholesterol efflux, and LCAT-mediated esterification in mice expressing the human cholesteryl ester transfer protein (CETP) and human apolipoprotein A-I (apoA-I) transgenes. J Lipid Res, 1996; 37:1268-1277
33) Miida T, Yamaguchi T, Tsuda T, and Okada M: High preβ1-HDL levels in hypercholesterolemia are maintained by probucol but reduced by a low-cholesterol diet. Atherosclerosis, 1998; 138:129-134
34) Rye KA and Barter PJ: Formation and Metabolism of prebeta-migrating, lipid-poor apolipoprotein A-I. Arterioscler Thromb Vasc Biol, 2004; 24:421-428